Article

SOURCE DATA | TRANSPARENT PROCESS

THE EMBO JOURNAL

LPS targets host guanylate-binding proteins to the bacterial outer membrane for non-canonical inflammasome activation

José Carlos Santos[1,2], Mathias S Dick[1], Brice Lagrange[3], Daniel Degrandi[4], Klaus Pfeffer[4], Masahiro Yamamoto[5], Etienne Meunier[6], Pawel Pelczar[7], Thomas Henry[3] & Petr Broz[1,2,*]

Abstract

Pathogenic and commensal Gram-negative bacteria produce and release outer membrane vesicles (OMVs), which present several surface antigens and play an important role for bacterial pathogenesis. OMVs also modulate the host immune system, which makes them attractive as vaccine candidates. At the cellular level, OMVs are internalized by macrophages and deliver lipopolysaccharide (LPS) into the host cytosol, thus activating the caspase-11 non-canonical inflammasome. Here, we show that OMV-induced inflammasome activation requires TLR4-TRIF signaling, the production of type I interferons, and the action of guanylate-binding proteins (GBPs), both in macrophages and *in vivo*. Mechanistically, we find that isoprenylated GBPs associate with the surface of OMVs or with transfected LPS, indicating that the key factor that determines GBP recruitment to the Gram-negative bacterial outer membranes is LPS itself. Our findings provide new insights into the mechanism by which GBPs target foreign surfaces and reveal a novel function for GBPs in controlling the intracellular detection of LPS derived from extracellular bacteria in the form of OMVs, thus extending their function as a hub between cell-autonomous immunity and innate immunity.

Keywords caspase-11; guanylate-binding proteins (GBPs); inflammasome; LPS; outer membrane vesicles

Subject Categories Immunology

DOI 10.15252/embj.201798089 | Received 25 August 2017 | Revised 17 January 2018 | Accepted 19 January 2018 | Published online 19 February 2018

The EMBO Journal (2018) 37: e98089

Introduction

Outer membrane vesicles (OMVs) are released by both pathogenic and commensal Gram-negative bacteria as part of their normal growth (Kaparakis-Liaskos & Ferrero, 2015; Schwechheimer & Kuehn, 2015). Proteomic and biochemical analysis has shown that they contain a variety of bacterial components from the outer Gram-negative membrane, like lipopolysaccharide (LPS) and lipoproteins, periplasmic proteins, but also DNA and RNA. While initial reports described OMVs produced by *Vibrio cholerae* and *Neisseria meningitidis in vitro* (Chatterjee & Das, 1967; Devoe & Gilchrist, 1973), OMVs have since been also shown to be produced by bacteria during infection of the host, indicating that they might contribute to pathogenesis (Kaparakis-Liaskos & Ferrero, 2015). Indeed, OMVs were reported to confer resistance to antimicrobials and the complement system by acting as decoys or to promote the adaptation to bacteria within the host, such as by enabling biofilm formation (Kaparakis-Liaskos & Ferrero, 2015; Pathirana & Kaparakis-Liaskos, 2016). Importantly, OMVs can also act as vehicles for the direct delivery of virulence factors or microbe-associated molecular patterns (MAMPs) to host cells or even get internalized into host cells (Kesty *et al*, 2004; Bomberger *et al*, 2009; Chen *et al*, 2010; Kaparakis *et al*, 2010; Irving *et al*, 2014), as several studies have shown that OMVs are taken up by endocytosis (O'Donoghue & Krachler, 2016). The high concentration of MAMPs on OMVs allows them to trigger many host pattern recognition receptors (PRRs), such as the LPS sensor TLR4, or TLR2 and TLR9 signaling. *In vivo*, OMVs have thus been shown to promote the induction of pro-inflammatory cytokines and chemokines during infection with *Helicobacter pylori*, *Legionella pneumophila*, and other pathogens (Kaparakis *et al*, 2010; Kaparakis-Liaskos & Ferrero, 2015). Since OMVs activate an immune response while simultaneously delivering a number of potential membrane-associated antigens, they have attracted attention as vaccine platforms and OMV-based vaccines

1 Focal Area Infection Biology, Biozentrum, University of Basel, Basel, Switzerland
2 Department of Biochemistry, University of Lausanne, Epalinges, Switzerland
3 Centre International de Recherche en Infectiologie, Inserm U1111, CNRS, UMR 5308, Université Claude Bernard Lyon-1, Ecole Normale Supérieure, Lyon, France
4 Institute of Medical Microbiology and Hospital Hygiene, Heinrich-Heine-University Düsseldorf, Düsseldorf, Germany
5 Department of Immunoparasitology, Research Institute for Microbial Diseases, Osaka University, Osaka, Japan
6 Institute of Pharmacology and Structural Biology (IPBS), University of Toulouse, Toulouse Cedex 04, France
7 Center for Transgenic Models, University of Basel, Basel, Switzerland
*Corresponding author. Tel: +41 21 692 56 56; E-mail: petr.broz@unil.ch

for *N. meningitidis* have already been approved in several countries (Acevedo *et al*, 2014; van der Pol *et al*, 2015).

An unsolved problem of OMV-based strategies is their high content in LPS, which is highly toxic to the organism but at the same time required for OMV stability and immunogenicity (Acevedo *et al*, 2014). A recent study has shown that OMVs can deliver LPS into the cytosol of mouse macrophages and that this results in activation of caspase-11 (Vanaja *et al*, 2016). Caspase-11 and its human orthologs caspase-4/-5 are part of the so-called non-canonical inflammasome pathway, and act as cytosolic sensors for LPS during infections with Gram-negative bacteria (Kayagaki *et al*, 2011, 2013; Broz *et al*, 2012; Rathinam *et al*, 2012; Aachoui *et al*, 2013; Hagar *et al*, 2013; Shi *et al*, 2014). Direct binding of LPS results in the oligomerization and activation of these caspases (Shi *et al*, 2014), allowing them to cleave gasdermin-D and generate an N-terminal gasdermin-D fragment, which rapidly induces pyroptosis, a form of programmed necrotic cell death, by forming plasma membrane pores (Kayagaki *et al*, 2015; Shi *et al*, 2015; Aglietti *et al*, 2016; Ding *et al*, 2016; Liu *et al*, 2016; Sborgi *et al*, 2016). Caspase-11 activation also drives the release of pro-inflammatory cytokines, interleukin (IL)-1β and IL-18, by initiating the activation of the NLRP3 inflammasome, which is classified as a canonical inflammasome and thus involves the activation of caspase-1 instead of caspase-11. Caspase-1 also cleaves and activates gasdermin-D (Kayagaki *et al*, 2015; Shi *et al*, 2015), but also features the ability to convert IL-1β/-18 into their mature bioactive form. *In vivo*, caspase-11 has been shown to provide protection against bacterial infections (Aachoui *et al*, 2013), but also to cause lethality in a mouse model of endotoxemia (Hagar *et al*, 2013; Kayagaki *et al*, 2013). Thus, modulation of caspase-11 activity could provide means to control LPS toxicity.

Previous studies by us and others have shown that caspase-11 activation during infections with Gram-negative bacteria requires production of type I interferons (type I IFNs) and the induction of IFN-stimulated GTPases, such as the guanylate-binding proteins (GBPs) and interferon-regulated GTPases (IRGs; Meunier *et al*, 2014; Pilla *et al*, 2014; Man *et al*, 2016a). GBPs and IRGs function in cell-autonomous immunity and have been shown to target both vacuolar and cytosolic pathogens, such as *Toxoplasma gondii, Salmonella Typhimurium, Escherichia coli, Francisella novicida,* and *L. pneumophila* (Meunier *et al*, 2014, 2015; Pilla *et al*, 2014; Man *et al*, 2015, 2016a; Kravets *et al*, 2016; Feeley *et al*, 2017). GBPs targeting controls the recruitment of IRGB10 to pathogens and ultimately results in the destruction of the vacuolar and/or pathogen membranes (Meunier *et al*, 2014, 2015; Man *et al*, 2015, 2016a; Kravets *et al*, 2016). This process results in the release of MAMPs, such as LPS or DNA, which have been shown to activate caspase-11 or the AIM2 inflammasome, respectively. Importantly, recruitment of GBPs and IRGs has been shown to absolutely require live pathogens, as no GBPs have been shown to associate with heat- or PFA-inactivated bacteria (Meunier *et al*, 2014; Feeley *et al*, 2017). However, whether GBPs also promote the recognition of MAMPs contained within OMVs that access the cytosol has not been explored so far.

Here, we show that OMV-induced activation of caspase-11, pyroptotic cell death, and IL-1β release require the engagement of TLR4-TRIF signaling and the production of type I IFNs. While type I IFNs contribute to caspase-11 induction, their main function is to induce the expression of GBPs. Macrophages deficient in several mouse *Gbps* consequently show much reduced levels of caspase-11 activation and pyroptosis. Mechanistically, we show that GBPs do not promote the entry of OMVs into the cytosol, but directly target cytosolic OMVs to promote caspase-11 activation, which requires GBP isoprenylation. Mimicking OMV-based LPS delivery using liposome-based transfection reagents demonstrated that even transfected LPS is targeted by GBPs. Furthermore, we show that the lipid A moiety of LPS is sufficient in determining GBP-dependent caspase-11 activation and that GBPs facilitate the interaction of LPS with caspase-11. Consistent with the requirement for GBPs *in vitro*, we show that GBP deficiency reduces the pro-inflammatory response caused by OMVs *in vivo* and promotes survival in a model of OMV-induced endotoxemia. Our data reveal a novel function for GBPs in controlling the intracellular detection of LPS derived from extracellular bacteria in the form of OMVs, thus extending their function as a hub between cell-autonomous and innate immunity.

Results

OMVs activate the non-canonical inflammasome in a TLR4-TRIF-dependent manner

Outer membrane vesicles were previously shown to deliver bacterial LPS into the host cytosol, thus triggering caspase-11 activation (Vanaja *et al*, 2016), but the requirement for other innate immune signaling pathways for this process remains to be addressed. As reported previously (Vanaja *et al*, 2016), we observed that unprimed bone marrow-derived macrophages (BMDMs) from wild-type mice underwent cell death [as measured by lactate dehydrogenase (LDH) release] and secreted mature IL-1β (ELISA) into the culture supernatant when treated with increasing amounts of OMVs purified from *E. coli* (Appendix Fig S1A–E). Cell death and cytokine release were completely abrogated in *Casp11*$^{-/-}$ BMDMs, indicating that *E. coli* OMVs only engage the non-canonical inflammasome pathway. Consistently, deficiency in *Nlrp3* abrogated the processing of pro-caspase-1 into the p20 subunit and the release of mature IL-1β and IL-18, but did not alter pyroptosis induction (Appendix Fig S1A, B, and D). Cell death and cytokine release were also completely dependent on gasdermin-D, the executor of pyroptotic cell death (Kayagaki *et al*, 2015; Shi *et al*, 2015; Sborgi *et al*, 2016; Appendix Fig S1A and E). Moreover, OMVs purified from other Gram-negative bacteria, such as *Pseudomonas aeruginosa*, *S. Typhimurium* (WT and Δ*orgA/fliC/fljAB),* and *Shigella flexneri,* also induced pyroptotic cell death and IL-1β release in a caspase-11-dependent manner (Appendix Fig S1F and G), demonstrating that activation of the non-canonical inflammasome is a common mechanism of OMVs from different, if not all Gram-negative bacteria.

Caspase-11 activation by intracellular Gram-negative bacteria requires the engagement of the TLR4–TRIF axis (Broz *et al*, 2012; Rathinam *et al*, 2012). Similarly, OMVs failed to induce pyroptosis and subsequent caspase-1 activation in *Tlr4*$^{-/-}$ and *Trif*$^{-/-}$ BMDMs, whereas *MyD88* deficiency had no influence on cell death and caspase-1 processing (Fig 1A and B). Since caspase-11 is only expressed following priming of BMDMs, we speculated that TRIF signaling is necessary for caspase-11 induction. However, while some reduction in caspase-11 expression was observed in *Tlr4*$^{-/-}$ BMDMs, we found comparable levels of caspase-11 in wild-type,

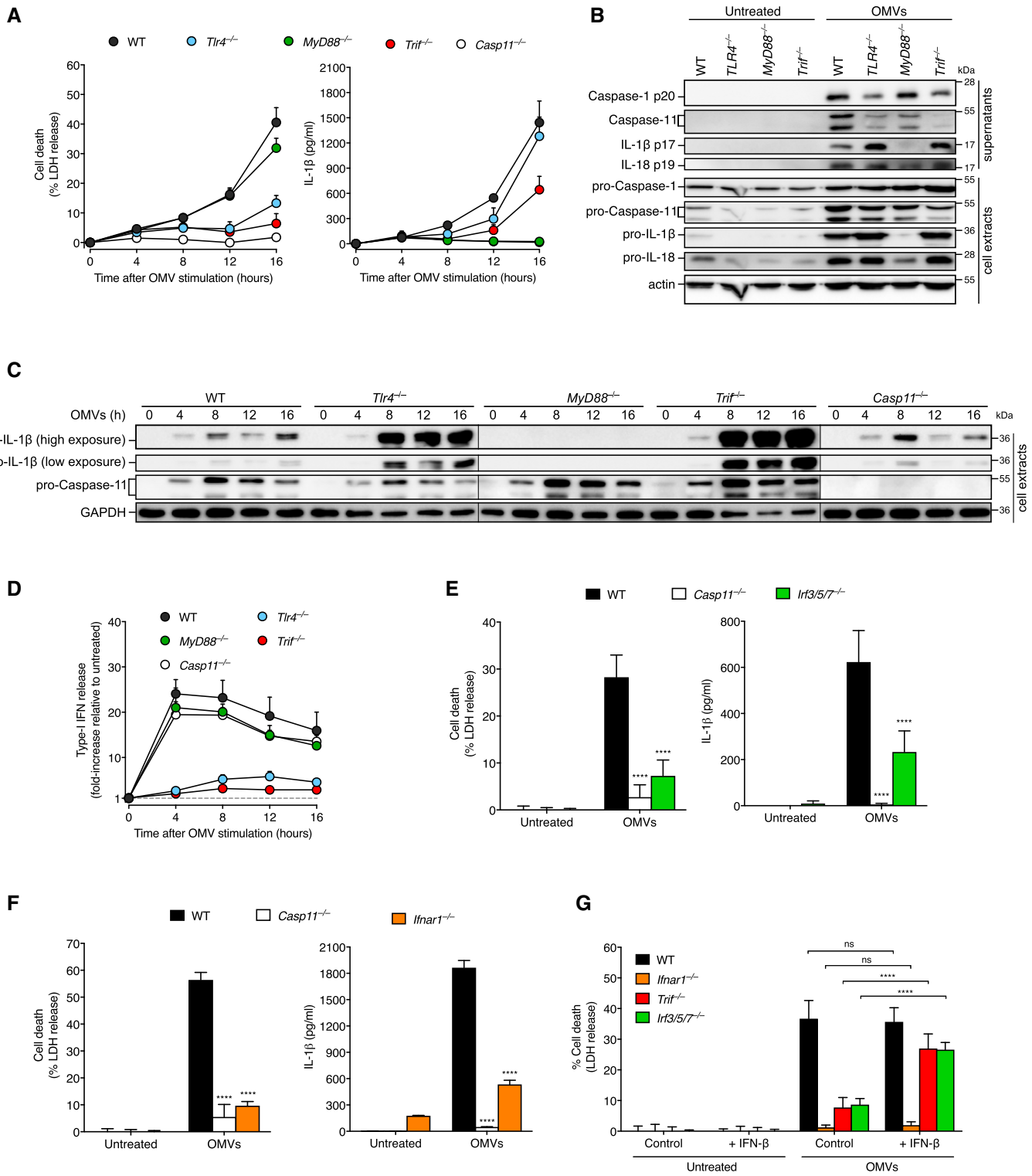

Figure 1.

Trif$^{-/-}$, and *MyD88*$^{-/-}$ BMDMs following stimulation with *E. coli* OMVs (Fig 1C), indicating that as previously reported TLR-TRIF plays a minor role in caspase-11 induction (Broz *et al*, 2012).

Unexpectedly, we observed that deficiency in *Tlr4* and *Trif* reduced IL-1β release only at early time points (4, 8, and 12 h; Fig 1A) and that at 16 h post-OMV treatment *Tlr4*$^{-/-}$ and *Trif*$^{-/-}$ BMDMs released similar or even higher levels of mature IL-1β than wild-type cells (Fig 1A and B). The most likely explanation for the increased IL-1β production is the negative regulatory effect exerted by type I IFNs on pro-IL-1β induction and canonical inflammasome

Figure 1. OMV-induced activation of the non-canonical inflammasome requires TLR4-TRIF-induced type I IFN signaling.

A Release of LDH and IL-1β from unprimed wild-type (WT), *Tlr4*$^{-/-}$, *MyD88*$^{-/-}$, *Trif*$^{-/-}$, and *Casp11*$^{-/-}$ BMDMs, at the indicated time points after treatment with OMVs purified from *Escherichia coli* BL21.

B Western blot analysis of cleaved caspase-1 (p20), caspase-11, IL-1β (p17), and IL-18 (p19) in cell supernatants, and of pro-caspase-1, pro-caspase-11, pro-IL-1β, pro-IL-18, and β-actin (loading control) in cell extracts of unprimed WT, *Tlr4*$^{-/-}$, *MyD88*$^{-/-}$, *Trif*$^{-/-}$, and *Casp11*$^{-/-}$ BMDMs, 16 h after treatment with purified *E. coli* OMVs.

C Induction of pro-IL-1β and pro-caspase-11 in unprimed BMDMs treated with purified *E. coli* OMVs for the indicated time points. Two different exposures (low and high) are shown for pro-IL-1β.

D Release of type I IFNs from unprimed WT, *Tlr4*$^{-/-}$, *MyD88*$^{-/-}$, *Trif*$^{-/-}$, and *Casp11*$^{-/-}$ BMDMs, 16 h after treatment with purified *E. coli* OMVs. Type I IFNs were measured using ISRE-L929 reporter cells, and data are presented as fold-increase relative to untreated control cells.

E, F Release of LDH and IL-1β from unprimed WT, *Casp11*$^{-/-}$, and *Irf3/5/7*$^{-/-}$ BMDMs (E) or WT, *Casp11*$^{-/-}$ and *Ifnar1*$^{-/-}$ BMDMs (F), 16 h after treatment with purified *E. coli* OMVs.

G Release of LDH in WT, *Ifnar1*$^{-/-}$, *Trif*$^{-/-}$, and *Irf3/5/7*$^{-/-}$ BMDMs treated with vehicle control or 1,000 U ml^{-1} recombinant mouse IFN-β and purified *E. coli* OMVs for 16 h.

Data information: Graphs show the mean and s.d., and data are pooled from three independent experiments (A, D–G) performed in triplicates or are representative from two (B and C) independent experiments. ****$P < 0.0001$, two-way analysis of variance test.
Source data are available online for this figure.

activation, as previously reported (Guarda *et al*, 2011). Consistent with this hypothesis, we found that pro-IL-1β expression was strongly increased in both *Tlr4*$^{-/-}$ and *Trif*$^{-/-}$ BMDMs upon stimulation with *E. coli* OMVs, compared to wild-type cells (Fig 1C). On the other hand, IL-1β secretion was significantly reduced in *MyD88*-deficient macrophages throughout the timecourse (Fig 1A and B). Moreover, pro-IL-1β expression required MyD88-dependent signaling, but not TRIF (Broz *et al*, 2012; Fig 1C). Overall, these data indicated that OMV-induced caspase-11 activation requires a TRIF-dependent signal and that TRIF signaling is not linked to the induction of caspase-11.

Type I IFN signaling is required for OMV-induced activation of the non-canonical inflammasome

The adaptor molecule TRIF controls activation of nuclear factor-κB (NF-κB) and interferon regulatory factor 3 (IRF3)-dependent production of type I IFNs downstream of TLR3 and TLR4 (Takeuchi & Akira, 2010). We first determined whether OMV stimulation induces type I IFN release in BMDMs (Fig 1D). Type I IFN release increased quickly within 4 h after OMV treatment, independently of MyD88 and caspase-11, but in a TLR4- and TRIF-dependent manner. Next, we investigated whether type I IFN signaling is required for activation of the non-canonical inflammasome upon *E. coli* OMV stimulation, by comparing cell death and IL-1β release in wild-type, *Casp11*$^{-/-}$, and *Irf3/5/7*$^{-/-}$ BMDMs (Fig 1E). Both cell death and IL-1β release were significantly reduced in *Irf3/5/7*$^{-/-}$ macrophages, suggesting an important role for type I IFN production in caspase-11 activation upon OMV stimulation. To further confirm this finding, we assessed inflammasome activation in cells lacking the interferon-α/β receptor alpha chain (*Ifnar1*$^{-/-}$). OMV-stimulated *Ifnar1*-deficient cells also showed reduced cell death and IL-1β release (Fig 1F). Furthermore, the requirement for type I IFN production and signaling upon OMV stimulation is exclusively dependent on TRIF and IRF3 signaling, given that macrophages deficient in STING —via the "goldenticket" (Gt) *N*-ethyl-*N*-nitrosourea-induced nonfunctional mutation of alleles encoding *Tmem173* (hereafter called *Sting*$^{Gt/Gt}$; Sauer *et al*, 2011)—did not show impaired inflammasome activation (Appendix Fig S2). To further corroborate that OMV-induced caspase-11 activation requires type I IFN signaling, macrophages were simultaneously treated with OMVs and recombinant mouse IFN-β. Addition of exogenous IFN-β restored pyroptotic cell death in *Trif*$^{-/-}$ and *Irf3/5/7*$^{-/-}$ macrophages, but not in *Ifnar1*$^{-/-}$ macrophages (Fig 1G). Moreover, macrophages treated with IFN-β did not induce cell death in the absence of OMV stimulation, confirming that IFN-β alone does not activate the non-canonical inflammasome. Taken together, our data reveal that OMVs induce type I IFN production, through TLR4 and TRIF signaling, and that signaling via IFNAR1 is necessary to trigger the activation the non-canonical inflammasome in response to intracellular OMVs.

GBPs promote OMV-dependent activation of the non-canonical inflammasome

Activation of the interferon-α/β receptor by type I IFNs induces expression of hundreds of interferon-stimulated genes (ISGs), and the products of many ISGs are important for innate immune activation and/or exert anti-microbial effects (Man *et al*, 2016b; Meunier & Broz, 2016). Prominent among ISG gene products are several families of interferon-inducible GTPases, such as the 65- to 73-kDa GBPs and the 45-kDa IRGs, which have been shown to target intracellular pathogens and their vacuoles, and ultimately promote their destruction and the release of MAMPs, such as LPS and DNA (Meunier *et al*, 2014, 2015; Man *et al*, 2015; Kravets *et al*, 2016). We observed that OMV stimulation of BMDMs induced upregulation of several *Gbps*, mostly *Gbp2* and *Gbp5* (Appendix Fig S3A). In addition, these two GBPs, which have been linked to anti-bacterial immunity (Meunier *et al*, 2014, 2015), were found to be strongly induced at the protein level in OMV-treated BMDMs, which required signaling through TRIF and IFNAR1 (Appendix Fig S3B). This is in accordance with previous reports that showed that these proteins are upregulated upon infection with Gram-negative bacteria (Meunier *et al*, 2014, 2015; Man *et al*, 2015, 2016a). Since stimulation with LPS and IFN-γ also induces GBP expression (Meunier *et al*, 2014; Appendix Fig S3C), we assessed whether priming accelerates inflammasome activation in response to OMVs. LPS and IFN-γ primed BMDMs released LDH and IL-1β as soon as 4 h after OMV stimulation, whereas naïve cells showed delayed inflammasome activation (Fig 2A), indicating that GBP induction accelerates

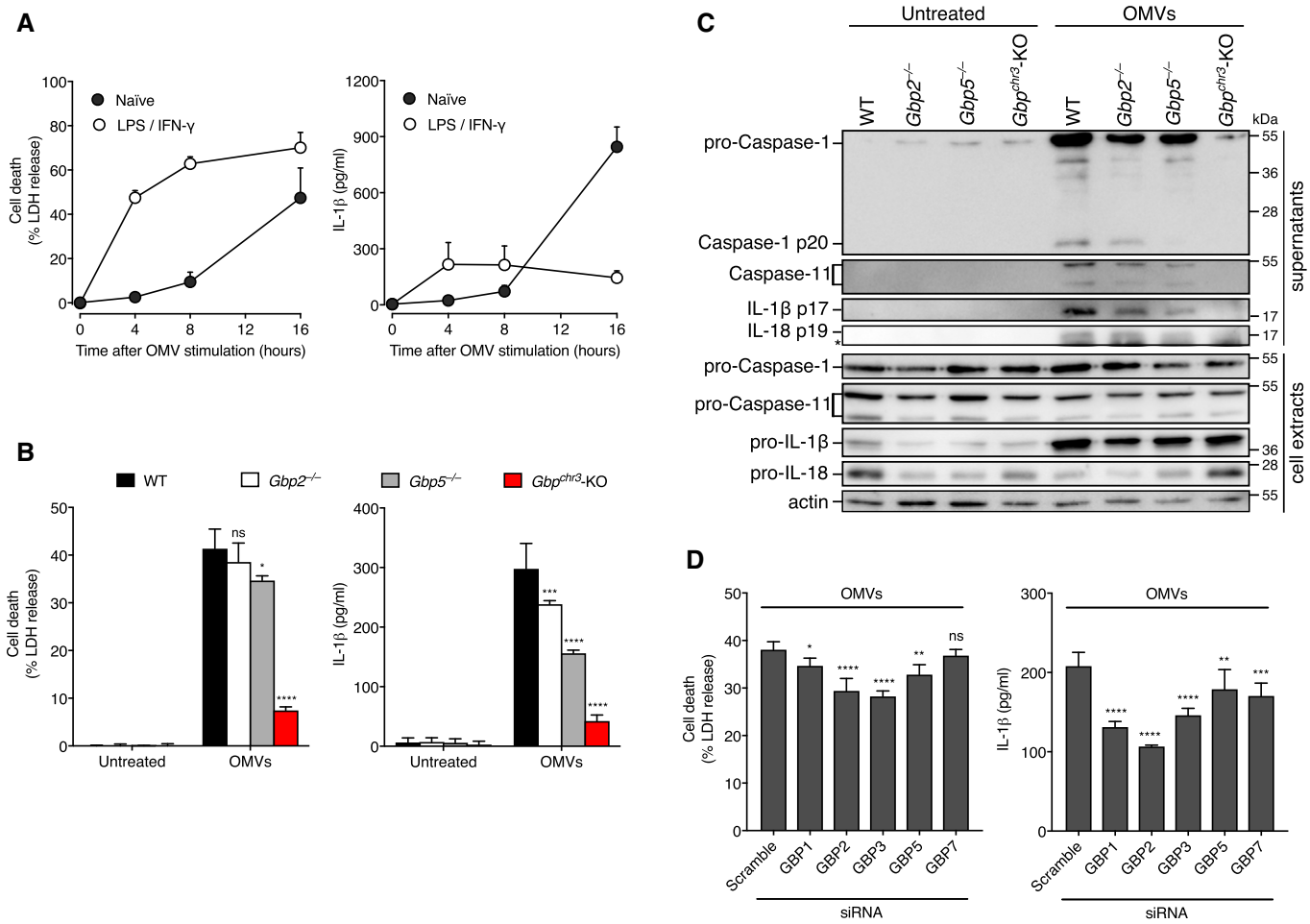

Figure 2. GBPs promote OMV-dependent non-canonical inflammasome activation.

A, B Release of LDH and IL-1β from naïve or LPS- and IFN-γ-primed WT BMDMs, at the indicated time points after treatment with *Escherichia coli* OMVs (A), or from LPS- and IFN-γ-primed WT, *Gbp2*$^{-/-}$, *Gbp5*$^{-/-}$, and *Gbp*^{chr3}-KO BMDMs, 4 h after treatment with *E. coli* OMVs (B).

C Western blot analysis of pro-caspase-1 and cleaved caspase-1 (p20), caspase-11, IL-1β (p17) and IL-18 (p19) in cell supernatants, and of pro-caspase-1, pro-caspase-11, pro-IL-1β, pro-IL-18, and β-actin (loading control) in cell extracts, of LPS- and IFN-γ-primed WT, *Gbp2*$^{-/-}$, *Gbp5*$^{-/-}$, and *Gbp*^{chr3}-KO, 4 h after treatment with purified *E. coli* OMVs.

D Release of LDH and IL-1β 4 h after stimulation with *E. coli* OMVs from LPS- and IFN-γ-primed BMDMs transfected with non-targeting scramble siRNA or with siRNAs targeting different GBPs for 72 h.

Data information: Graphs show the mean and s.d., and data are pooled from three independent experiments performed in triplicate (A and B) or are representative of two independent experiments (C) or of three independent experiments performed in quadruplicate (D). *$P < 0.05$, **$P < 0.01$, ***$P < 0.001$, ****$P < 0.0001$, two-way analysis of variance test.
Source data are available online for this figure.

OMV-dependent activation of the non-canonical inflammasome. Interestingly, naïve cells released more mature IL-1β than primed cells at 16 h post-OMV stimulation, most likely because IFN-γ-induced signaling negatively regulates TLR4-dependent pro-IL-1β expression (Appendix Fig S3C) and the delayed cell death allows for an accumulation of pro-IL-1β.

We then asked whether GBPs are required for OMV-induced activation of the non-canonical inflammasome. Wild-type, *Gbp2*$^{-/-}$, *Gbp5*$^{-/-}$, or *Gbp*^{chr3}-KO (deficient for the locus on mouse chromosome 3 encoding GBP1, GBP2, GBP3, GBP5, and GBP7) BMDMs were primed with LPS and IFN-γ, to induce GBP expression, and then stimulated with OMVs for 4 h. *Gbp*^{chr3}-deficient macrophages showed an almost complete reduction in cell death, and in the release of IL-1β (even comparable to *Casp11*$^{-/-}$ BMDMs: Appendix Fig S3D), caspase-1 p20 and caspase-11, when compared to wild-type cells (Fig 2B and C). Interestingly, *Gbp2*- and *Gbp5*-deficient cells released comparable levels of LDH as wild-type controls, but had partially decreased levels of cytokine release, suggesting that besides GBP2 and GBP5, other GBPs on mouse chromosome 3 might contribute as well. To identify these, we used RNA interference to individually knock down *Gbp1, 2, 3, 5,* or *7* expression in BMDMs, before treating the cells with *E. coli* OMVs. Yet, GBPs appeared to be redundant, since single knock-down of *Gbp1, 2, 3,* or *5* only reduced cell death and cytokine release partially, while the knock-down of *Gbp7* had no significant effect (Fig 2D). We also tested the role of GBPs on chromosome 3 for the activation of the non-canonical inflammasome

upon stimulation with OMVs from different Gram-negative bacteria. As seen for *E. coli* OMVs, Gbp^{chr3}-deficient macrophages also showed impaired cell death and IL-1β release after stimulation with *Pseudomonas*, *Salmonella,* or *Shigella* OMVs (Appendix Fig S3E and F). Together with the previous data, these findings suggest that OMV-associated LPS induces GBP expression through TLR4/TRIF-dependent type I IFN production and that several different GBPs are required to induce activation of the caspase-11 non-canonical inflammasome in response to intracellular OMVs.

GBPs do not control cytosolic localization of OMVs

Next, we tried to get insights into the mechanisms by which GBPs control caspase-11-dependent sensing of OMV-derived LPS. As previously described (Vanaja *et al*, 2016), OMV-dependent inflammasome activation requires clathrin-mediated endocytosis, given that the inhibitors dynasore (dynamin inhibitor) and chlorpromazine (CPZ; clathrin-mediated endocytosis inhibitor) impaired cell death and IL-1β release in macrophages (Fig 3A). Fluorescence confocal microscopy of wild-type and Gbp^{chr3}-KO BMDMs treated with OMVs that have been pre-labeled with a lipophilic fluorescent dye showed that OMVs localized to early endosomes, as soon as 30 min after internalization (Fig 3B and Appendix Fig S4A). Moreover, by 3 h after stimulation, most OMVs seemed to be in a non-endosomal compartment or within the host cytosol. We then asked whether GBPs control internalization of OMVs into cells. To address this, we stimulated wild-type and Gbp^{chr3}-KO cells with fluorescent OMVs for different time points and quantified the percentage of cells containing intracellular OMVs by fluorescence microscopy. By 10 min, about 30% of cells contained intracellular OMVs, and this percentage increased to a maximum of about 70% by 3 h after stimulation. The percentage of intracellular OMVs was, however, the same in both wild-type and Gbp^{chr3}-deficient cells (Fig 3C), indicating that GBPs do not control the endocytosis of OMVs.

Outer membrane vesicle-derived LPS was shown to get access to the cytosol from the early endosomes (Vanaja *et al*, 2016). Therefore, we next assessed whether GBPs on chromosome 3 could be implicated in OMV accessibility to the host cytosol, for example, by promoting destabilization of the endosomal membrane, similarly to the destabilization of pathogen-containing vacuoles (PCVs; Meunier *et al*, 2014). For this, we isolated OMVs from bacteria expressing β-lactamase ($OMVs^{β\text{-}lact}$) and we used a sensitive FRET-reporter assay that takes advantage of the cleavable cephalosporin-derived probe CCF4 that can be loaded into the host cytoplasm (Fig 3D, left panel). If $OMVs^{β\text{-}lact}$ gain access the cytosol of macrophages and release β-lactamase, the FRET reporter is hydrolyzed, which leads to a loss of FRET and a switch of fluorescence emission from green to blue upon excitation of the probe at 405 nm (Ray *et al*, 2010; Keller *et al*, 2013). Briefly, wild-type and Gbp^{chr3}-KO BMDMs were loaded with the CCF4 FRET reporter, stimulated with $OMVs^{β\text{-}lact}$, and the loss of FRET signal (as determined by the ratiometric measurement of the 450/520 nm intensities) was assessed over time. We found that GBPs did not seem to play a role in OMV accessibility to the host cytosol, as we could not observe a significant difference in the loss of FRET between wild-type and Gbp^{chr3}-KO macrophages (Fig 3D, right panel). As expected, $OMVs^{β\text{-}lact}$ accessibility to the host cytosol required prior endocytosis of OMVs as it was blocked by dynasore treatment. To rule out that the increase in the loss of FRET was due to OMV lysis and consequent release of β-lactamase, the CCF4 reporter was incubated *in vitro* in the presence or absence of $OMVs^{β\text{-}lact}$. This showed that intact $OMVs^{β\text{-}lact}$ release sufficient amounts of β-lactamase to hydrolyze the probe (Appendix Fig S4B).

Finally, we also determined whether GBPs affect the amount of LPS found in the host cytosol. For that, we extracted the cytosol from untreated or OMV-stimulated wild-type and Gbp^{chr3}-KO BMDMs, using a differential digitonin fractionation protocol (Ramsby & Makowski, 2011), and determined the levels of LPS using the limulus amebocyte lysate (LAL) assay. The use of a low digitonin concentration (0.01%) for a short period of time allowed us to extract a cytosolic fraction that was devoid of contaminations with other organelles, namely lysosomes, endoplasmic reticulum (ER), and mitochondria (Appendix Fig S4C). Moreover, the fractionation procedure does not seem to induce damage of intracellular membrane-bound compartments, given that PDI, a protein resident in the ER lumen, was not found in the cytosolic fraction. In accordance with a recent report (Vanaja *et al*, 2016), we found that LPS was only present in the cytosolic and not in the residual, non-cytosolic fraction of OMV-treated macrophages (Fig 3E), yet Gbp^{chr3}-deficient cells contained the same levels of cytosolic LPS as wild-type cells (Fig 3E). Together, these data suggest that GBPs do not play a role in OMV endocytosis or in the accessibility of OMVs or OMV-derived LPS from the endosome to the macrophage cytosol.

Figure 3. GBPs do not mediate OMV-derived LPS access to the host cytosol.

A Release of LDH and IL-1β from LPS- and IFN-γ-primed BMDMs pre-treated with different endocytosis inhibitors and then stimulated with *Escherichia coli* OMVs for 4 h.

B Fluorescence confocal microscopy of wild-type and Gbp^{chr3}-KO BMDMs stimulated with OMVs pre-labeled with Vybrant DiI (red) and fixed at the indicated time points. Early endosomes were labeled using an anti-EEA-1 antibody (green), and nuclei were stained with Hoechst (blue). Representative confocal images are shown. Scale bars correspond to 5 μm.

C Wild-type (WT) and Gbp^{chr3}-KO BMDMs were stimulated with OMVs pre-labeled with Vybrant DiI, cells were fixed at the indicated time points, and the percentage of cells with intracellular fluorescent OMVs was quantified by confocal microscopy, by counting at least 50 cells per coverslip.

D To evaluate OMV access to the host cytosol, WT and Gbp^{chr3}-KO BMDMs were loaded with CCF4-AM FRET substrate and stimulated with $OMVs^{β\text{-}lact}$. The loss of FRET signal (as determined by the ratiometric measurement of the 450/520 nm intensities) was assessed at the indicated time points, using a plate reader. In parallel, BMDMs pre-treated with the endocytosis inhibitor dynasore were used as a control.

E LPS quantification (LAL assay, EU ml^{-1}) in the cytosol and residual fractions of digitonin-fractionated WT and Gbp^{chr3}-KO BMDMs after stimulation with 50 μg of *E. coli* OMVs for 2 h.

Data information: Graphs show the mean and s.d., and data are pooled from three (A) or two (C and E) independent experiments performed in triplicate or are representative of two (B) or three (D) independent experiments performed in triplicate. ***$P < 0.001$, ****$P < 0.0001$, two-tailed *t*-test (E) or two-way analysis of variance test (A and D).

Isoprenylation is required for the association of GBP5 with OMVs and non-canonical inflammasome activation

Guanylate-binding protein function appears to be closely linked to their ability to associate with PCVs or cytosolic pathogens; however, what part of the pathogen is recognized is unclear. A recent study used structured illumination microscopy on cytosolic *E. coli* to analyze GBP localization, revealing that a layer of IRGB10 co-localized or closely associated with a layer of GBP5, both encased by a layer of LPS (Man *et al*, 2016a). We therefore treated BMDMs with

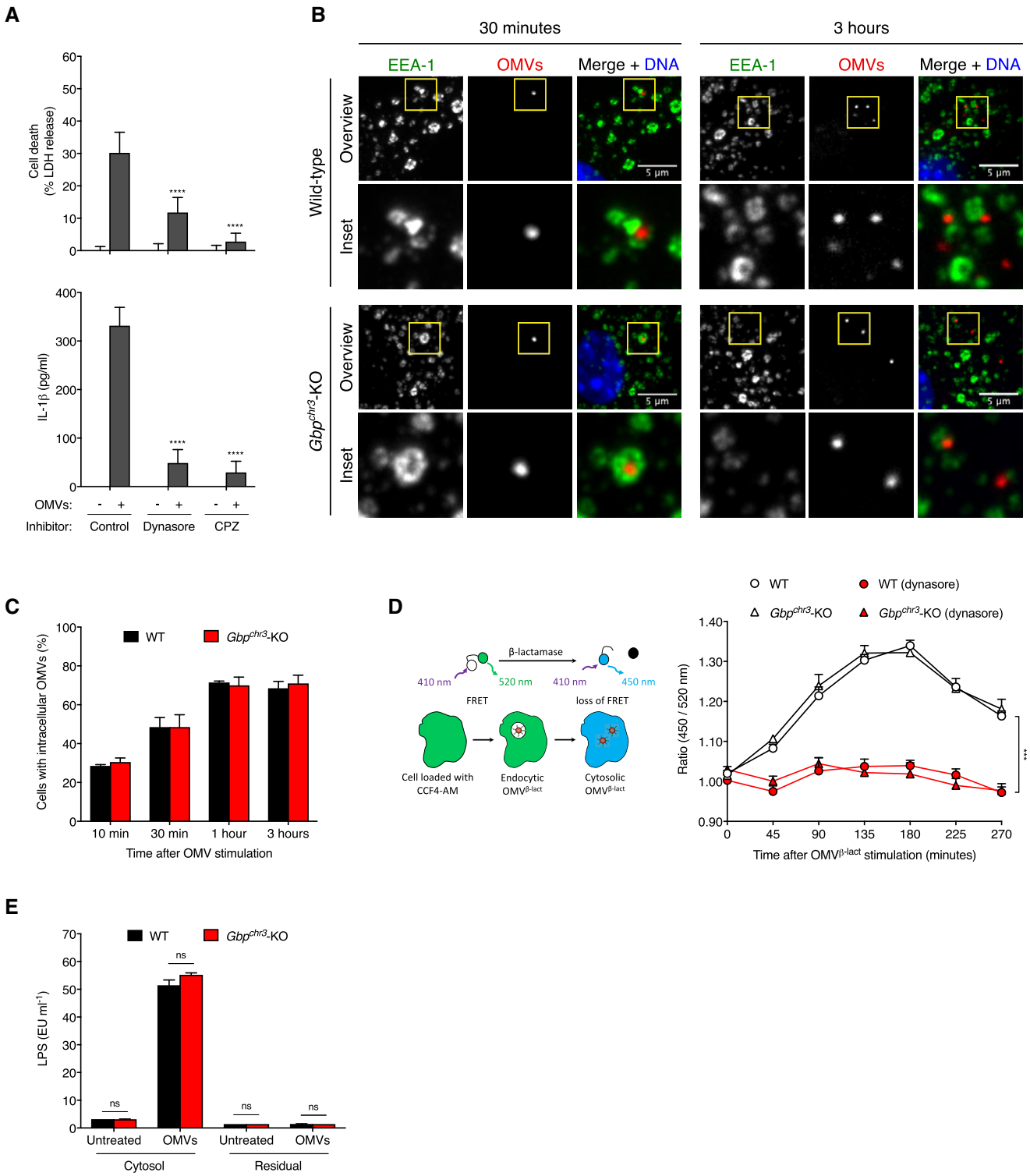

Figure 3.

fluorescently labeled OMVs and analyzed them for GBP5 co-localization by immunofluorescence and confocal microscopy. OMVs were rapidly targeted by GBP5, and by 1 h after internalization, approximately 70% of OMVs were found to stain positive for GBP5, which was not observed in *Gbp*^{chr3}- or *Gbp5*-deficient BMDMs (Fig 4A–C). Interestingly, the association of GBP5 with OMVs decreased again at 3 h post-treatment, suggesting that the interaction was transient (Fig 4C). Importantly, this decrease was observed in WT as well as *Casp11*- and *Gsdmd*-deficient cells, confirming that the reduction in OMV-GBP5 association was not caused by loss of cells through pyroptosis (Fig 4C). We next assessed whether several GBPs are recruited to intracellular OMVs by using U937 cells stably expressing HA-tagged human GBP1, 2, or 5. Treatment of these cells confirmed the results obtained for GBP5 in BMDMs and showed that human GBP5, GBP1, and GBP2 also associate with intracellular OMVs (Fig 4B, and details on Appendix Fig S4D). Since OMVs are devoid of the peptidoglycan layer or the inner bacterial membrane, our data suggest that the critical factor of Gram-negative bacteria that drives GBP recruitment is found within the outer bacterial membrane.

Several GBPs are characterized by the presence of a carboxyl-terminal "CaaX" motif for isoprenylation (Kim *et al*, 2016). Mutation of this motif disrupts the ability of GBPs to associate with endomembranes, and, for example, the C586S mutant of GBP2 loses its ability to target the *Toxoplasma*-containing vacuole and to restrict parasite replication (Kravets *et al*, 2016). We therefore investigated whether isoprenylation was necessary for GBP recruitment to OMVs and for non-canonical inflammasome activation by treating BMDMs with a farnesyl transferase inhibitor (FTI), which blocks isoprenylation (Modiano *et al*, 2005), prior to stimulation with OMVs. Immunofluorescence analysis revealed that association of GBP5 with intracellular OMVs required protein isoprenylation, as it was inhibited by FTI treatment (Fig 4D). Indirect or secondary effects of the inhibitor on GBP induction could be ruled out, since FTI treatment did not impair expression of *Gbp1*, *2*, *3*, *5*, or *7* (Appendix Fig S4E), or release of type I IFN (Appendix Fig S4F) in primed BMDMs. To further demonstrate that GBP isoprenylation is required for targeting of cytosolic OMVs, we generated U937 cells stably expressing HA-tagged ΔCaaX-GBP1, 2, or 5. We then treated these cells with fluorescently labeled OMVs and assessed recruitment of GBPs. In accordance with our data using the FTI treatment in BMDMs, human ΔCaaX-GBP5 also showed impaired association with intracellular OMVs (Fig 4E), while no significant reduction in association could be observed for ΔCaaX-GBP1 or ΔCaaX-GBP2. Decreased ΔCaaX-GBP5 association with intracellular OMVs, when comparing to wild-type GBP5, was not due to diminished protein expression (Appendix Fig S4G). Finally, we examined whether FTI treatment had an impact on caspase-11 activation in OMV-treated cells. FTI incubation prior to stimulation with OMVs significantly reduced non-canonical inflammasome activation (Fig 4F), but had no effect on *Casp11* induction (Appendix Fig S4E). As a control, cells were also treated with nigericin, which ruled out secondary effects of FTI treatment on NLRP3 activation (Fig 4E). Overall, these data show that GBPs require isoprenylation to target cytosolic OMVs and that the recruitment of GBPs to OMVs is necessary to drive LPS recognition by caspase-11.

LPS is the critical component of the bacterial outer membrane that drives GBP recruitment

Our data and previous reports (Meunier *et al*, 2015; Man *et al*, 2016a) suggest that the bacterial surface is targeted by GBPs, yet the bacterial ligand/factor that determines GBP recruitment is unknown. Since LPS is the main constituent of OMVs, we examined whether LPS is necessary and sufficient to drive GBP recruitment to the bacterial outer membrane. To investigate this notion, we used LPS transfection, which results in the incorporation of LPS in liposomal vesicles that can, at least to some extent, mimic OMV structure and that are also delivered to the cytosol via the endocytic route. In accordance with previous results (Pilla *et al*, 2014), GBPs were necessary for caspase-11 activation at early time points after LPS transfection (Fig 5A), but interestingly, this GBP dependency disappeared over the course of time (Appendix Fig S5A), as we had observed before (Meunier *et al*, 2014; Pilla *et al*, 2014). As observed with OMV, single deficiency in GBP2 or GBP5 only slightly reduced cytokine release and cell death, while *Gbp*^{chr3}-KO cells showed significant reduction (Fig 5A). It is worth noting that caspase-11 activation by LPS transfection and OMV treatment were comparably GBP^{chr3}-dependent (Figs 2B and 5A), indicating that proteins found in OMVs contributed little to GBP-dependent caspase-11 activation. GBP dependency appeared not to be linked to the route of delivery of transfected or OMV-delivered LPS (via endocytosis), since we did not observe any requirement for GBPs^{chr3} when transfecting poly (dA:dT) (Fig 5B), as observed previously (Man *et al*, 2015; Meunier *et al*, 2015).

Since inflammasome activation upon delivery of LPS by transfection or through OMVs were both GBP^{chr3} dependent, we asked whether GBPs targeted cytosolic transfected LPS. Interestingly, GBP5

Figure 4. GBPs association with OMVs and inflammasome activation require protein isoprenylation.

A Fluorescence confocal microscopy of wild-type, *Gbp*^{chr3}-KO, and *Gbp5*$^{-/-}$ BMDMs stimulated with OMVs pre-labeled with Vybrant Dil (red) for 1 h and immunostained for GBP5 (green). The nucleus was stained with Hoechst (blue). Squares and respective inset images show intracellular OMVs intracellular OMVs. Representative confocal images are shown. Scale bars correspond to 1 or 10 μm.

B Fluorescence confocal microscopy in U937 cells expressing HA-tagged GBP1, GBP2, or GBP5 and treated with OMVs with Vybrant Dil (red) for 1 h. GBPs were labelled using an anti-HA antibody (green), and the nucleus was stained with Hoechst (blue). Scale bars correspond to 5 μm.

C, D Percentage of GBP5-positive OMVs, as quantified by counting at least 50 intracellular OMVs per coverslip by confocal microscopy, in WT, *Gbp*^{chr3}-KO, *Casp11*$^{-/-}$, and *Gsdmd*$^{-/-}$ BMDMs (C), or in control and FTI-treated WT BMDMs (D), stimulated with pre-labeled OMVs and fixed at the indicated time points.

E Percentage of OMVs positive for wild-type (wt) or ΔCaaX HA-tagged human GBP1, GBP2 or GBP5 in U937 cells. At least 50 intracellular OMVs were counted per coverslip, using confocal microscopy, 1 h upon stimulation of cells with pre-labeled OMVs.

F Release of LDH and IL-1β from LPS- and IFN-γ-primed control or FTI-treated wild-type BMDMs, 4 h after stimulation with *E. coli* OMVs or 2 h after treatment with 20 μM nigericin.

Data information: Graphs show the mean and s.d. Data are representative of three independent experiments performed in triplicate (A and B) or are pooled from two (E) or three (C, D, and F) independent experiments performed in triplicate. $^{**}P < 0.01$, $^{***}P < 0.001$, two-tailed *t*-test (D and E) or two-way analysis of variance test (F).

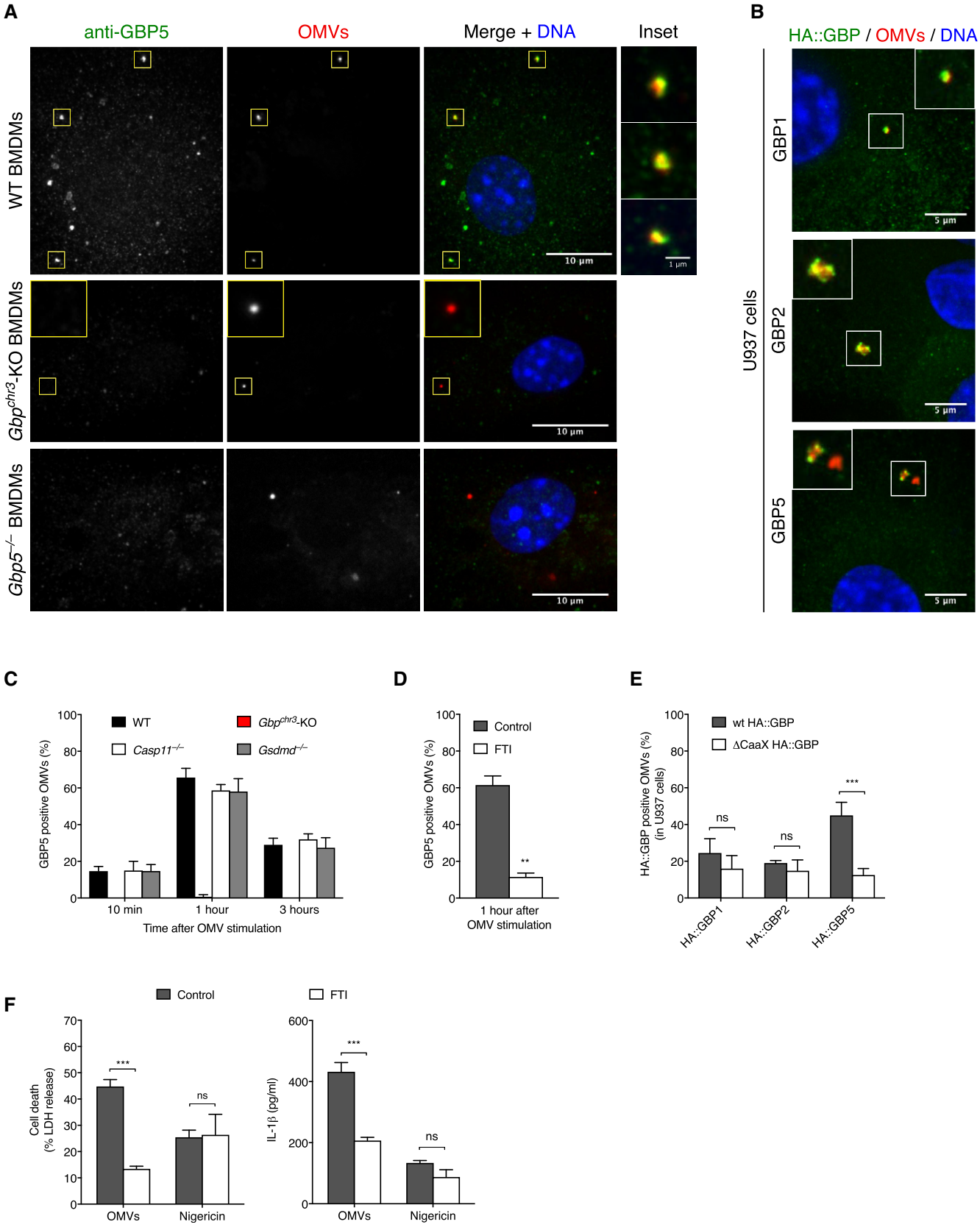
A
anti-GBP5
OMVs
Merge + DNA
Inset
WT BMDMs
Gbp^chr3-KO BMDMs
Gbp5^-/- BMDMs
10 μm
1 μm
B
HA::GBP / OMVs / DNA
U937 cells
GBP1
GBP2
GBP5
5 μm
C
WT
Gbp^chr3-KO
Casp11^-/-
Gsdmd^-/-
GBP5 positive OMVs (%)
10 min
1 hour
3 hours
Time after OMV stimulation
D
Control
FTI
GBP5 positive OMVs (%)
1 hour after OMV stimulation
E
wt HA::GBP
ΔCaaX HA::GBP
HA::GBP positive OMVs (%) (in U937 cells)
ns
***
HA::GBP1
HA::GBP2
HA::GBP5
F
Control
FTI
Cell death (% LDH release)
IL-1β (pg/ml)
OMVs
Nigericin

Figure 4.

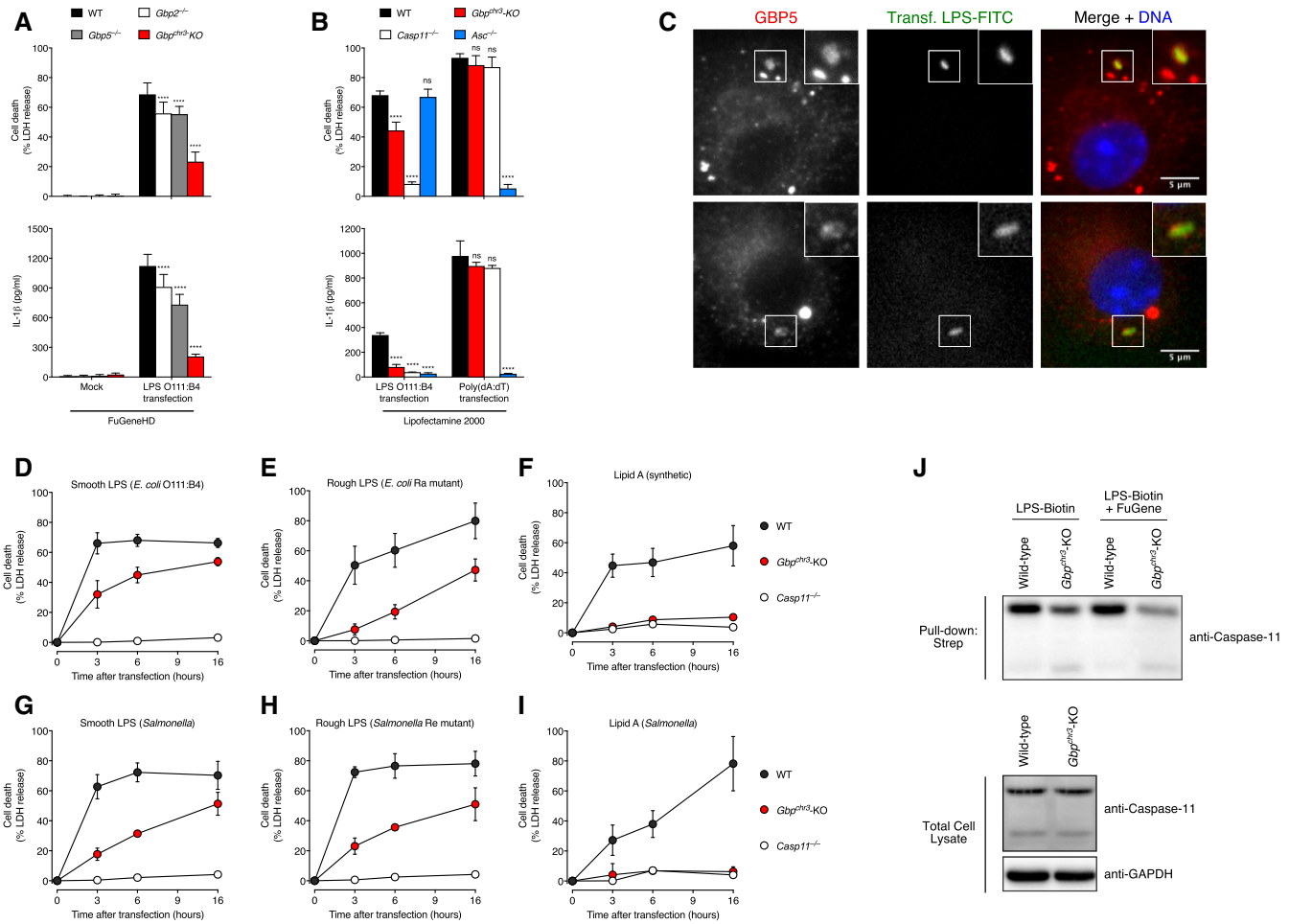

Figure 5. Lipid A determines GBP-dependent caspase-11 activation upon LPS transfection.

A Release of LDH and IL-1β from LPS- and IFN-γ-primed WT, *Gbp2*$^{-/-}$, *Gbp5*$^{-/-}$, and *Gbp*^{chr3}-KO BMDMs, 2 h after LPS transfection (using FuGeneHD).

B Release of LDH and IL-1β from LPS- and IFN-γ-primed WT, *Gbp*^{chr3}-KO, *Casp11*$^{-/-}$, and *Asc*$^{-/-}$ BMDMs 2 h after transfection with LPS or poly(dA:dT), using Lipofectamine 2000.

C Fluorescence confocal microscopy of wild-type BMDMs transfected with LPS-FITC for 1 h and immunostained for GBP5 (red). The nucleus was stained with Hoechst (blue). Squares and respective inset images show GBP5 association with intracellular LPS. Representative confocal images are shown. Scale bars correspond to 5 µm.

D–I Release of LDH from LPS- and IFN-γ-primed WT, *Gbp*^{chr3}-KO, and *Casp11*$^{-/-}$ BMDMs at different time points after transfection with *E. coli* O111:B4 LPS (D), *E. coli* rough LPS (E), synthetic lipid A (F), *S. minnesota* smooth LPS (G), *S. minnesota* rough LPS (H), or *S. minnesota* lipid A (I), using FuGeneHD.

J Streptavidin pulldown assay of the binding of biotin-conjugated LPS to endogenous caspase-11 from the lysates of wild-type (WT) and *Gbp*^{chr3}-KO BMDMs. Cells were primed with LPS and IFN-γ, and 700 µg of total cell lysate was incubated with 2.0 µg LPS-biotin or with 2.0 µg LPS-biotin pre-mixed with FuGeneHD. Pulldown of biotinylated LPS was performed using equal amounts of streptavidin magnetic beads, which were eluted in equal volumes of SDS–PAGE reducing sample buffer. Shown are anti-caspase-11, anti-GBP5, and anti-GAPDH immunoblots of the pulldowns and total cell lysates.

Data information: Graphs show the mean and s.d., and data are representative of three (C) or four (J) independent experiments, or are pooled from three independent experiments performed in triplicate (A, B, D–I). ****$P < 0.0001$, two-way analysis of variance test.
Source data are available online for this figure.

was found to associate with transfected ultrapure FITC-labeled LPS (Fig 5C). To rule out unspecific association of GBP5 with the transfection reagent or with FuGeneHD-bound endogenous lipoproteins, we also transfected BMDMs with Pam_3CSK_4-Rhodamine, a synthetic triacylated lipopeptide that mimics the acylated amino terminus of bacterial lipoproteins. Transfected Pam_3CSK_4-Rhodamine reached the host cytosol to a similar extent as LPS-FITC (Appendix Fig S5B), but was only poorly targeted by GBP5 (Appendix Fig S5C). When co-transfecting cells with a mixture of LPS-FITC and Pam_3CSK_4-Rhodamine, the double-positive LPS/Pam_3CSK_4 gets targeted by GBP5 to the same degree as LPS-FITC transfection alone (Appendix Fig S5C). This strongly suggests that LPS is the critical component of the bacterial outer membrane that drives the recruitment of GBPs. LPS consists of the lipid A moiety, core oligosaccharides, and the O-linked polysaccharides (also referred to as O-antigen). Lipid A is the minimal unit necessary for TLR4 or caspase-11 activation, but which part/s of LPS are necessary for promoting GBP-dependent activation of caspase-11 is unknown. We therefore transfected smooth LPS (e.g., O111:B4), rough LPS (*E. coli* Ra mutant, lacking O-antigens), or lipid A (lacking O-antigen and core oligosaccharides)

from *E. coli* into WT and Gbp^{chr3}-KO cells and monitored activation of the non-canonical inflammasome over time. Of note, since lipid A is the minimal unit necessary for caspase-11 interaction, all these types of LPS trigger non-canonical inflammasome activation. At early time points after transfection (3 h), all types of LPS activated caspase-11 in a GBP^{chr3}-dependent manner. Surprisingly, however, we found that with time the dependency on GBP^{chr3} decreased for smooth or rough LPS transfection, while lipid A-induced caspase-11 remained fully GBP^{chr3}-dependent at all time points (Fig 5D–F), even up to 16 post-transfection. Similarly, we found that lipid A from *S. minnesota* activated caspase-11 in a manner absolutely dependent on GBP^{chr3}, while GBPs were only partially required for caspase-11 activation induced by smooth or rough (Re mutant, lipid A + KDO) *S. minnesota* LPS (Fig 5G–I). In addition, we also purified OMVs from different *E. coli* strains that lack specific enzymes in the LPS biosynthetic pathway and therefore have distinct LPS structures (Appendix Fig S5D). In accordance with the previous data, we observed that upon BMDM stimulation with these different OMVs, GBP^{chr3}-dependent caspase-11 activation decreases over time (Appendix Fig S5E–G). Altogether our data suggest that the key factor of the Gram-negative outer bacterial membrane that promotes GBP recruitment is LPS itself or the presence of LPS in a target membrane and that the lipid A moiety of LPS is sufficient for this process.

GBPs promote caspase-11 binding to bacterial LPS

Our data indicate that GBPs are recruited to LPS-containing membranes and that this is required for activation of the non-canonical inflammasome. This suggests that GBPs can then actively function as intermediate players between LPS and caspase-11. Caspase-11 is known to directly and specifically bind to LPS (Shi *et al*, 2014), which is important to activate caspase-11 and consequent pyroptosis. Moreover, it seems that this interaction is mediated by the lipid A moiety of LPS (Shi *et al*, 2014). However, lipid A is highly hydrophobic and embedded within the bacterial outer membrane, which raises a fundamental question as how can it interact with caspase-11, a cytosolic protein. We therefore hypothesized that additional host factors such as GBPs could participate and help lipid A/LPS binding to caspase-11. To test this, we prepared cell lysates from wild-type and Gbp^{chr3}-KO BMDMs, which were then incubated with biotinylated LPS. After subsequent pulldown with streptavidin-coupled beads, we compared the levels of endogenous caspase-11 bound to LPS. As seen in Fig 5J, we found that in the absence of GBPs caspase-11 bound less efficiently to LPS. Moreover, and in order to mimic LPS-containing membranes, we incubated cell lysates with biotinylated LPS that has been pre-mixed with FuGeneHD transfection reagent, which results in incorporation of LPS in the liposomal vesicle. This resulted in a more dramatic decrease in caspase-11 binding to LPS in the absence of GBPs (Fig 5J). Together, these data suggest that GBPs facilitate caspase-11 binding to intracellular LPS, mostly when LPS is incorporated within liposomal membranes and possibly within the bacterial outer membrane as well.

GBP deficiency protects against OMV-induced lethal endotoxemia *in vivo*

To investigate the relevance of our *in vitro* findings *in vivo*, we next first determined the response of C57BL/6 mice to OMV challenge. Wild-type and Gbp^{chr3}-KO animals were injected intra-peritoneally with 100 μg of purified *E. coli* OMVs, and the plasma cytokine levels were assayed by multiplex array at 6 h post-injection (Fig 6A and Appendix Fig S6A). OMV-challenged animals displayed a strong pro-inflammatory signature characterized by elevated levels of IL-1α/-β, -5, -6, -17, TNF-α and IFN-γ, as well as chemokines MCP-1, MIP-1α, MIP-1β, and RANTES. As expected from our *in vitro* results, we observed strongly reduced levels of inflammasome-dependent cytokines, IL-1β and IL-18, in OMV-challenged Gbp^{chr3}-KO animals. Notably, however, we found that many other cytokines were also significantly reduced in Gbp^{chr3}-KO animals, suggesting that GBPs play an important role in regulating the general production of pro-inflammatory cytokines and chemokines, possibly by controlling the levels of IL-1β/-18 release. Consistent with our *in vitro* data, we also observed significantly elevated levels of plasma type I IFNs at 3 and 5 h post-OMV injection (Fig 6B). We next asked whether *in vivo* IL-1β and IL-18 production required GBPs and the non-canonical inflammasome, by comparing plasma cytokine levels in wild-type, $Casp11^{-/-}$, $Gsdmd^{-/-}$, or Gbp^{chr3}-KO mice primed with poly(I:C) and treated with OMVs (Fig 6C and Appendix Fig S6B). Consistent with a crucial role for caspase-11 in sensing OMV-derived LPS *in vivo*, we observed that $Casp11^{-/-}$ mice display very low levels of plasma IL-1β and IL-18 compared to wild-type mice. While IL-1β and IL-18 levels in Gbp^{chr3}-KO mice were not as strongly reduced as in $Casp11^{-/-}$ animals, they were still significantly lower than in wild-type mice, indicating that GBPs regulate the inflammasome-dependent cytokine production *in vivo*. OMV injection did not only elicit a strong pro-inflammatory response but also resulted in rapid lethality (Fig 6D), presumably due to LPS-induced endotoxemia. We therefore assessed whether the non-canonical inflammasome and GBPs were required for OMV-induced lethality *in vivo*. Poly(I:C)-primed wild-type, $Casp11^{-/-}$, and Gbp^{chr3}-KO mice were injected with OMVs, and survival was monitored for 5 days. Consistent with the sepsislike pro-inflammatory response (Fig 6A) and published reports, we found that OMV challenge induced lethality in wild-type mice with similar kinetics as previously reported for LPS-induced endotoxic shock (Fig 6D; Hagar *et al*, 2013; Kayagaki *et al*, 2013). Both *Casp11*- and *Gsdmd*-deficient animals survived OMV challenge (Fig 6D and Appendix Fig S6C), indicating that OMV-induced lethality was dependent on the cytosolic detection of LPS by the non-canonical inflammasome and subsequent induction of cell death by gasdermin-D. Gbp^{chr3}-KO mice were partially protected from OMV-induced lethality as the animals died later and around 50% survived OMV challenge. In addition, when mice were injected with purified LPS at 5 mg kg^{-1} body weight, we observed a higher survival rate in Gbp^{chr3}-KO animals, when compared to wild-type mice (Fig 6E). These results support the notion that GBPs on mouse chromosome 3 control activation of caspase-11 and gasdermin-D *in vivo*, and thus promote endotoxic shock induced by OMV-derived LPS.

Discussion

Guanylate-binding proteins are increasingly recognized as an essential part of IFN-dependent cell-autonomous immunity, thanks to an impressive number of recent studies. Here, we show that GBPs have a central role in controlling non-canonical

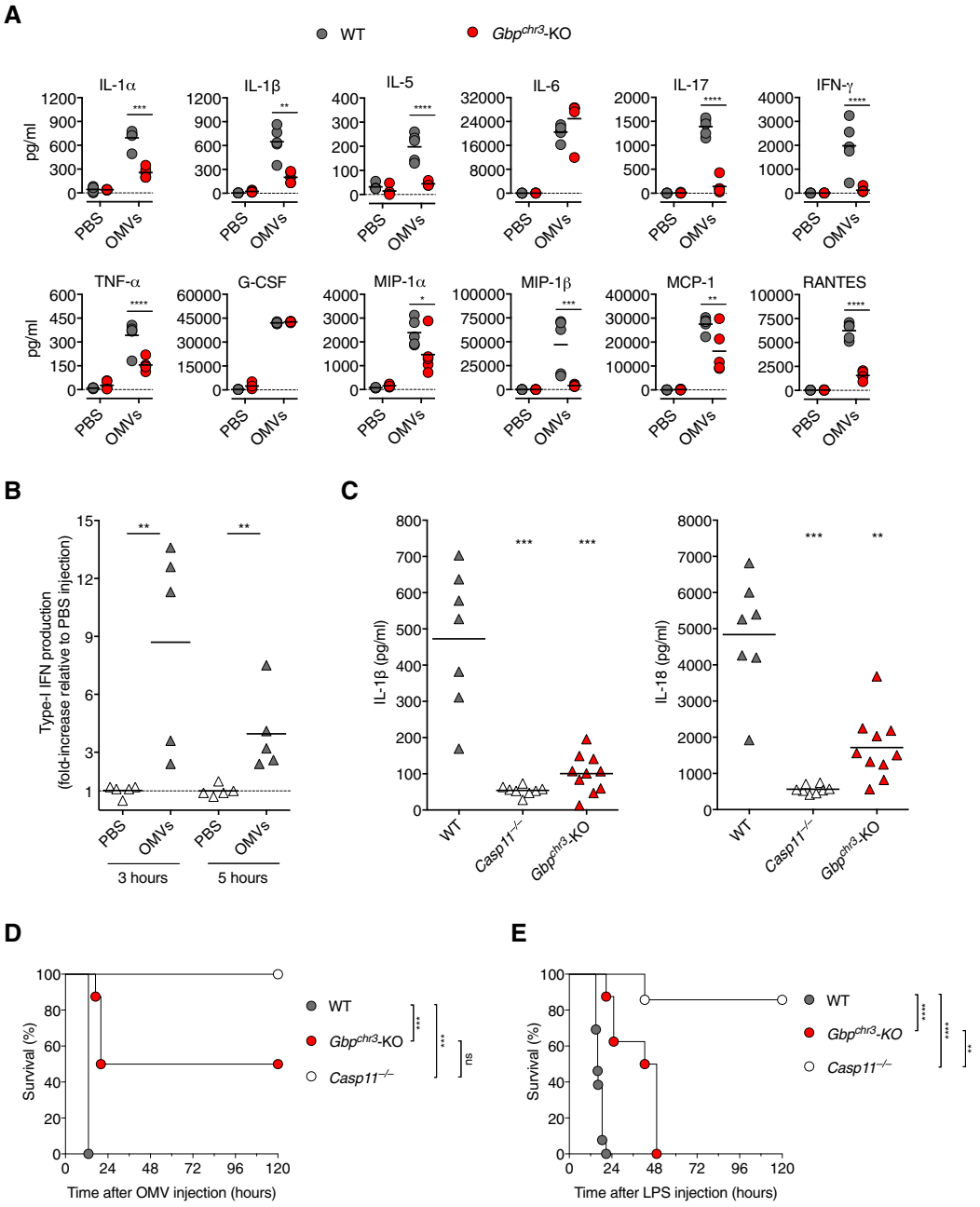

Figure 6. GBPs are necessary for OMV-induced endotoxic shock *in vivo*.

A Cytokine and chemokine levels in the plasma of wild-type (WT) and *Gbp*^{chr3}-KO mice injected i.p. with PBS or 100 μg of *E. coli* OMVs for 5 h (n = 5 animal per condition).

B Levels of type I IFNs in the plasma of WT mice injected i.p. with PBS or 100 μg of *E. coli* OMVs for 3 or 5 h. Type I IFNs were measured using ISRE-L929 reporter cells, and data are presented as fold-increase relative to PBS injected mice (n = 5 animals per condition).

C IL-18 and IL-1β levels in the plasma of WT, *Casp11*$^{-/-}$ and *Gbp*^{chr3}-KO mice primed with 200 μg poly(I:C) for 6 h and injected i.p. with 100 μg of *E. coli* OMVs for 5 h [n = 7 (WT), 8 (*Casp11*$^{-/-}$) or 10 (*Gbp*^{chr3}-KO) animals].

D, E Survival of WT, *Casp11*$^{-/-}$ and *Gbp*^{chr3}-KO mice primed with 200 μg poly(I:C) for 6 h and i.p. injected with 100 μg of *E. coli* OMVs [D, n = 8 (WT), 8 (*Gbp*^{chr3}-KO) or 6 (*Casp11*$^{-/-}$) animals] or 5 mg kg^{-1} LPS [E, n = 13 (WT), 8 (*Gbp*^{chr3}-KO) or 8 (*Casp11*$^{-/-}$) animals].

Data information: In (A–C), each symbol represents an individual mouse and the small horizontal lines indicate the mean. Data are representative of two independent experiments (B–E) or were performed with five individual mice per condition (A). *P < 0.05, **P < 0.01, ***P < 0.001, ****P < 0.0001, Mann-Whitney test (A–C) or log-rank Cox-Mantel test (D and E).

inflammasome activation and LPS-induced endotoxic shock in response to cytosolic bacterial OMVs. While this manuscript was under review, this role of GBPs was also reported by Coers *et al* (Finethy *et al*, 2017). Although a number of these studies report the association of GBPs with PCVs, cytosolic bacteria, or parasites (Meunier *et al*, 2014, 2015; Man *et al*, 2015, 2016a; Kravets *et al*,

2016), the factor/s that drives GBP recruitment have remained unknown. Prompted by the finding that even internalized bacterial OMVs are targeted by GBPs and trigger GBP-dependent caspase-11 activation in BMDMs (Fig 7), we investigated which part of OMVs is necessary for this process. Unexpectedly, our data indicate that LPS, the main constituent of the bacterial outer membrane, is sufficient to promote GBPs recruitment.

These findings trigger a number of questions, in particular if the interaction of LPS and GBPs is direct or through intermediate proteins. It is possible that LPS forms membrane micro-domains that proficiently allow the membrane insertion of isoprenylated GBPs, such as GBP1, -2, and -5. On the other hand, it is also possible that GBPs directly interact with LPS itself. However, since we find that lipid A is the critical part of LPS that allows GBP

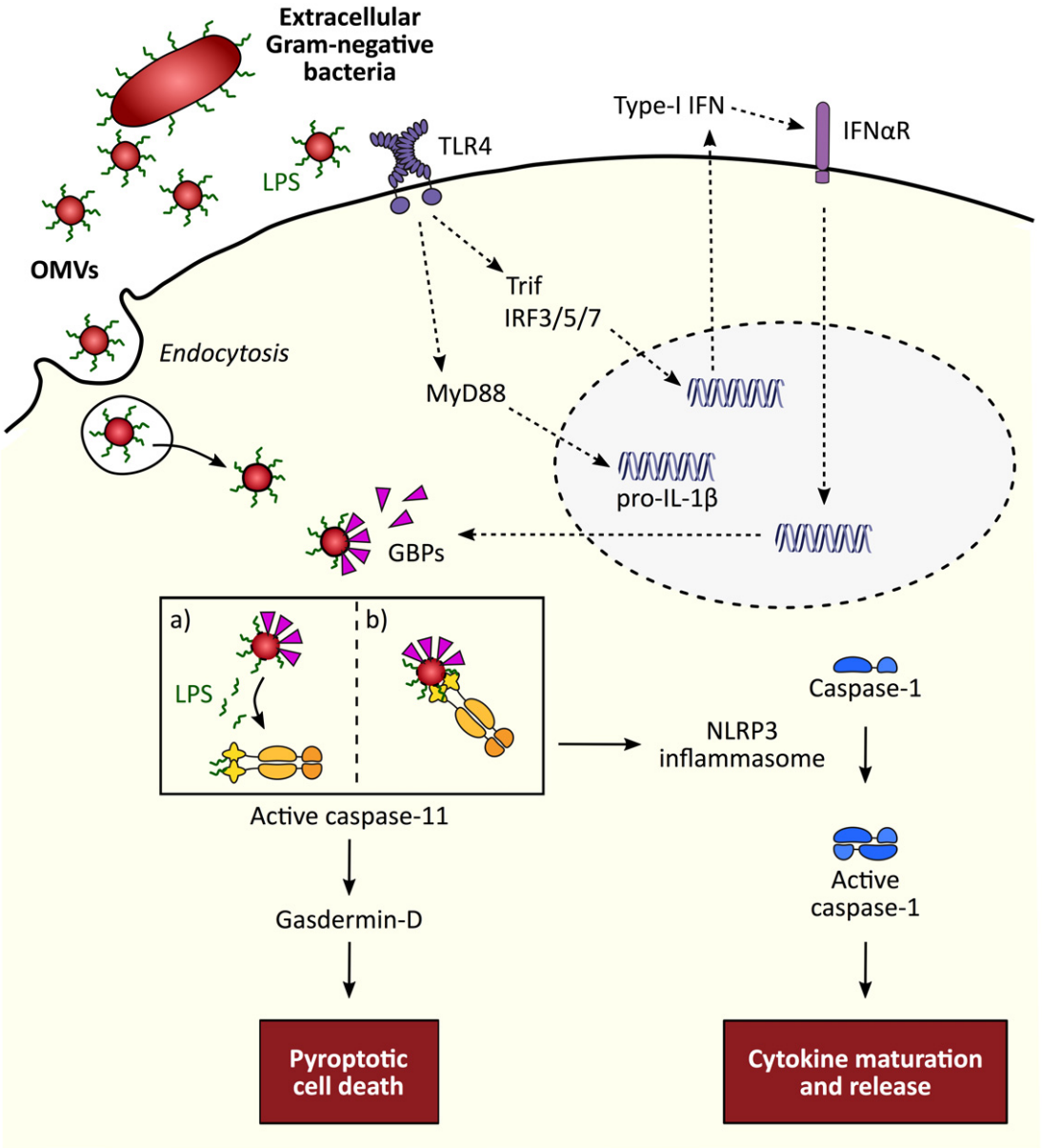

Figure 7. Model for the role of GBPs in OMV-mediated caspase-11 activation.

Outer membrane vesicles released by extracellular Gram-negative bacteria are internalized by macrophages via clathrin-mediated endocytosis. OMV-derived LPS is then released from the early endosome into the host cytosol, by a yet-unknown mechanism. In parallel, extracellular OMVs activate TLR4, via LPS, which triggers MyD88-dependent expression of pro-IL-1β. Activated TLR4 also induces TRIF activation, initiating a signaling cascade that activates IRF3 and results in the expression and release of type I IFNs. Type I IFNs signal in an autocrine and paracrine manner, through IFNAR, to induce expression of GBPs. The presence of LPS within the OMV membrane then results in the recruitment of GBPs, either directly or indirectly with the help of additional proteins, such as galectin-3 (Feeley *et al*, 2017). Based on previous work, we hypothesize that OMV-associated GBPs promote the engagement of a membrane-disrupting activity, possibly by recruiting IRGB10 (Man *et al*, 2016a), which helps disrupting the LPS-containing bacterial outer membrane of OMVs. This could ultimately either (a) releases LPS and thus allows caspase-11 activation or (b) allow direct access of caspase-11 to the lipid A moiety of LPS within the OMV membrane.

recruitment, it is hard to determine how GBPs would gain access to the lipid A moiety since it is contained within the membrane. Additional experiments, such as pulldown using LPS or with purified GBPs, will be necessary to determine whether GBPs interact directly with LPS or through intermediate proteins. Furthermore, proteomics analysis of the LPS-GBP5-containing complex purified from WT cells or individual GBP knock-outs will be necessary to identify the components of GBP-containing complexes and to establish the hierarchy of GBP recruitment. Our data suggest that isoprenylation of the CaaX motif of human GBP5 is important for its interaction with bacterial outer membranes. Interestingly, GBP isoprenylation seems to be important only for association of human GBP5 with intracellular OMVs, which is not observed for human GBP1 and -2. This might suggest a hierarchical association of different GBPs with the bacterial outer membrane, in which human GBP5 could be the first player of a multi-molecular GBP complex.

Interestingly, a recent study by Coers *et al* suggests that galectin-3 interacts with GBP2 and that galectin-3 is necessary to recruit GBPs to the *L. pneumophila* vacuole following T3SS-induced damage (Feeley *et al*, 2017). But whether galectins are also involved in recruiting GBPs to the bacterial outer membrane has not been addressed. This is not entirely unlikely, since other studies have shown that galectin-3 and other galectin family members bind not only galactosides on ruptured vacuolar compartments, but also bacterial- and parasite-derived carbohydrates (Mey *et al*, 1996; Debierre-Grockiego *et al*, 2010; Fermino *et al*, 2011). Galectin-3, for example, can bind to β-galactoside-containing LPS via its C-terminal carbohydrate recognition domain, or interact with the lipid A/inner core region of *S. minnesota* LPS, which is devoid of β-galactosides, through its N-terminal domain (Mey *et al*, 1996). Such a galectin-3–lipid A interaction would be in line with our finding that even lipid A drives GBP-dependent caspase-11 activation. Further experiments will be necessary to confirm direct/indirect interaction between LPS and GBPs, and to determine whether galectins possibly recruit GBPs and GBP-associated anti-microbial defense mechanisms to pathogens or their vacuolar compartments.

A puzzling finding is that caspase-11 activation after transfection of smooth and rough LPS is only partially GBP^{chr3}-dependent and that this dependency decreases over time, whereas lipid A-induced caspase-11 activation remains strongly GBP^{chr3}-dependent at all time points. A possible explanation for these observations might be that LPS has a higher solubility than lipid A. The critical micellar concentration (CMC) of LPS is 22–30 μg ml^{-1}, whereas lipid A has a CMC of 10 μg ml^{-1} (Aurell & Wistrom, 1998). Thus, LPS-containing micelles or membranes have a higher tendency to release soluble monomers into the aqueous environment than lipid A-containing membranes, which might account for the gradual loss of GBP dependency with time following LPS transfection. Alternatively, it could be possible that additional host factors, such as the GBPs encoded on mouse chromosome 5 or unrelated proteins, promote caspase-11 activation in response to smooth LPS but not lipid A, which would also explain the transient requirement for GBP^{chr3} during smooth LPS-induced caspase-11 activation. The contribution of additional host factors for OMV-induced inflammasome activation might also explain why *in vivo* IL-1β production and IL-18 production in Gbp^{chr3}-KO animals were not as strongly reduced as in $Casp11^{-/-}$ mice. Moreover, this could account for the observed partial protection of Gbp^{chr3}-KO mice in response to OMV-induced lethality.

A major unanswered and controversial question is the function of GBPs after they are recruited to a target surface. Several groups, including us, have reported that GBPs restrict pathogen replication and that this is linked to a direct anti-microbial activity that results in the lysis of PCVs and direct killing of cytosolic pathogens (Meunier *et al*, 2014, 2015; Man *et al*, 2015, 2016a; Kravets *et al*, 2016). Indeed, live microscopy analysis of *Toxoplasma gondii* infected cells has visualized how GBPs attack and lyse the parasitophorous vacuole and revealed that this is followed by a direct attack of GBPs on the released pathogen itself (Kravets *et al*, 2016). Furthermore, GBP-positive bacteria often appear disrupted and loose membrane integrity (Meunier *et al*, 2014, 2015; Man *et al*, 2015, 2016a; Kravets *et al*, 2016). Whether GBPs exert this function themselves or assemble a platform on the bacterial surface that allows for the recruitment of anti-microbial proteins is so far unknown. It has also been reported that GBP recruitment results in the recruitment of IRG proteins, like IRGB10, that would lyse the pathogen membrane (Man *et al*, 2016a). This is, however, difficult to reconcile with other studies that suggest that autophagy proteins and IRGs control the recruitment of GBPs to the *Chlamydia trachomatis* inclusion (Haldar *et al*, 2014, 2015) or the fact that IRGs can only be found in mice but not in humans, whereas GBPs are conserved in both species.

Besides killing the cytosolic pathogens, it has also been proposed that GBP-induced lysis allows the access of cytosolic pattern recognition receptors to previously masked or inaccessible MAMPs like LPS or DNA, which would explain how GBPs control the activation of canonical and non-canonical inflammasomes during infection (Man *et al*, 2016b; Meunier & Broz, 2016). Alternatively, it has been proposed that GBPs are themselves part of inflammasome complexes, such as the NLRP3 or the non-canonical inflammasome (Shenoy *et al*, 2012; Pilla *et al*, 2014). Our finding that LPS promotes the close association of GBPs with pathogen membranes could indeed also be explained by a model in which GBPs form part of an LPS-sensing macromolecular complex that assembles on the bacterial outer membrane and that contains LPS, GBPs, and caspase-11. Indeed, it has been suggested that OMVs present LPS to human caspase-4 (Wacker *et al*, 2017), and caspase-11 has been found to localize to OMVs or even cytosolic bacteria (Thurston *et al*, 2016; Vanaja *et al*, 2016), although these preliminary observations will need independent confirmation and additional controls. As part of such a complex, GBPs could, for example, disrupt the outer bacterial membrane and help LPS, namely its lipid A moiety, to get more accessible for recognition by caspase-11. This could explain how GBPs promote caspase-11 binding to LPS, mostly when LPS is present in membrane interfaces. This would be in line with the observation that lipid A, which has lower CMC than LPS (Aurell & Wistrom, 1998), absolutely requires GBPs to activate caspase-11. Alternatively, it could also be speculated that GBPs directly interact with LPS and present it to caspase-11, similarly to LPS-binding protein or MD2 that promote TLR4-dependent recognition of extracellular LPS. Interestingly, the requirement for helper or co-receptor proteins is not universal and is dictated by the type of LPS that is sensed [for details see (Beutler *et al*, 2006)], as CD14, for example, is absolutely necessary for TLR4 signaling induced by smooth LPS, while lipid A can induce the recruitment of MyD88 even in the absence of CD14 (Jiang *et al*, 2005). A third possibility, in which GBPs would act as cytosolic LPS sensor, is rather unlikely since LPS can bind directly to caspase-11 and

induce its oligomerization *in vitro* (Shi *et al*, 2014). Nevertheless, at low LPS concentrations, additional factors such as GBPs might become necessary.

In conclusion, further studies will be necessary to further characterize how LPS-containing membranes interact with GBPs, how this interaction results in pathogen restriction and inflammasome activation, and which molecules promote the recruitment of GBPs to surfaces that do not contain any LPS, such as the membranes of PCVs or parasites.

Materials and Methods

Mice and bacterial strains

Casp11$^{-/-}$, *Nlrp3*$^{-/-}$, *Gsdmd*$^{-/-}$, *Tlr4*$^{-/-}$, *MyD88*$^{-/-}$, *Trif*$^{-/-}$, *Irf3/5/7*$^{-/-}$, *Ifnar1*$^{-/-}$, *Sting*$^{Gt/Gt}$ *Gbp*^{chr3}-KO, *Gbp2*$^{-/-}$, and *Gbp5*$^{-/-}$ mice have been previously described. *Gsdmd*$^{-/-}$ were created at the Center for Transgenic model of the University of Basel as follows: Guide RNAs targeting exon 2 of the mouse *Gsdmd* gene were designed as described (Kayagaki *et al*, 2015) using gRNA sequence (including PAM) GGAGAAGGGAAAATTTCTGG. Injection of the gRNAs and Cas9 protein into C57BL/6 embryos was done as described before (Hermann *et al*, 2014). Biopsies for genotyping were taken at an age of 10–12 days. DNA extraction was performed using the KAPA HotStart Mouse Genotyping Kit according to the manufacturer's protocol. Genotyping PCR was done using Q5 Polymerase (NEB) using primers Oligo.507 (GSDMD_ex2_fw2; ggttgtga gccaccgtctat) and Oligo.508 (GSDMD_ex_rv2; ctgtggagggactccattgt), which were designed using Primer3 v.0.4.0 giving a fragment of 768 bp. The PCR product was sequenced using Oligo.507. All mice were bred at the animal facility of the University of Basel. The following bacterial strains were used to purify OMVs: *Escherichia coli* BL21 and its isogenic Δ*rfaC* or Δ*rfaG* strains, *Pseudomonas aeruginosa* PAO1, *Salmonella* Typhimurium SL1344 and its isogenic Δ*orgA/fliC/fljAB* strain (lacking SPI-1, T3SS and flagellin) and *Shigella flexneri* M90T. OMVs containing β-lactamase were purified from *E. coli* BL21 expressing β-lactamase, which was obtained by transforming bacteria with a pcDNA3 plasmid conferring ampicillin resistance. Bacteria were grown in lysogeny broth (LB) at 37°C with constant agitation, with the exception of *Shigella flexneri*, which was grown in tryptic casein soy broth (TCSB).

Purification and characterization of bacterial OMVs

Bacteria were grown overnight, sub-cultured 1/1,000 in 500 ml of medium and cultured overnight. Bacteria-free supernatant was collected by centrifuging at 10,000 × *g* for 10 min at 4°C and filtered through a 0.45-μm filter. The supernatant was then filtered through a 0.22-μm filter to remove any remaining debris or bacteria, and OMVs were pelleted by ultracentrifugation at ~150,000 × *g* for 3 h at 4°C. After removing the supernatant, OMVs were pelleted in sterile PBS. Purified OMVs were subjected to agar plating to ensure absence of bacterial contamination, and the protein content of each OMV preparation was determined using the Pierce BCA protein assay kit (Thermo Scientific), according to the manufacturer's instructions. Purified OMVs were further processed for negative staining and transmission electron microscopy according to standard procedures.

Animal stimulation with OMVs or LPS

Approximately 10-week-old sex-matched mice were used for all experiments. C57BL/6 and *Gbp*^{chr3}-KO mice were intraperitonially (i.p.) injected with 100 μg of purified OMVs or PBS, and cytokine levels in the plasma were assessed by Mouse Cytokine Array/Chemokine Array 31-Plex (Eve Technologies Corporation, Canada). In the experiments where C57BL/6, *Casp11*$^{-/-}$, *Gbp*^{chr3}-KO, and *Gsdmd*$^{-/-}$ animals were compared, mice were first primed with i.p. administration of 200 μg of poly(I:C) (low molecular weight, Invivogen) for 6 h prior i.p. injection with 100 μg of purified OMVs (Vanaja *et al*, 2016). Cytokine levels in the plasma were assessed 6 h post-OMV injection. For survival experiments, mice were primed with i.p. administration of 200 μg of poly(I:C) (low molecular weight, Invivogen) for 6 h prior i.p. injection with 100 μg of purified OMVs or with 5 mg kg^{-1} body weight LPS from *E. coli* O111:B4 (Invivogen). Mice were then monitored for 5 days. All animal experiments were approved (license 2535, Kantonales Veterinäramt Basel-Stadt) and were performed according to local guidelines (Tierschutz-Verordnung, Basel-Stadt) and the Swiss animal protection law (Tierschutz-Gesetz).

Cell culture and OMV stimulation

Bone marrow-derived macrophages were differentiated in DMEM (Sigma) supplemented with 10% FCS (Bioconcept), 20% MCSF (L929 mouse fibroblast supernatants), 10 mM HEPES, and nonessential amino acids, as previously described (Broz *et al*, 2010). One day before the corresponding treatment, macrophages were seeded into 24- or 96-well plates at a density of 2.5 × 10^5 or 5 × 10^4 cells per well, respectively. U937 cells stably expressing HA-tagged GBPs were cultured in RPMI-1640 supplemented with 10% FCS. U937 cells were then differentiated for 48 h with 100 ng ml^{-1} PMA and seeded at a density of 2 × 10^5 cells per well in a 24-well plate. When indicated, cells were also primed overnight with 300 ng ml^{-1} LPS [from *E. coli* O111:B4 (Invivogen)] 10 ng ml^{-1} mouse IFN-γ (PeproTech), or 1,000 U ml^{-1} mouse IFN-β (R&D systems). BMDMs were treated with 10 μg OMVs per 50,000 cells in Opti-MEM, unless indicated otherwise. Plates were centrifuged for 5 min at 206 × *g*, to ensure similar OMV adhesion, and cells were incubated at 37°C for the indicated time points. Transfection of cells with poly(dA:dT) (Invivogen, 25 ng/50,000 cells) was done using Lipofectamine 2000 (Invitrogen) in Opti-MEM as previously described (Meunier *et al*, 2014). Transfection of cells with smooth LPS from *E. coli* O111:B4 (Invivogen), rough LPS from *E. coli* EH100 (Ra mutant; L9641; Sigma), smooth LPS from *S. minnesota* R595 (Invivogen), rough LPS from *S. minnesota* Re 595 (Re mutant; L9764; Sigma), monophosphoryl synthetic lipid A (ALX-581-205-C100; Enzo Life Sciences), and monophosphoryl lipid A from *S. minnesota* R595 (Invivogen) was done at a concentration of 500 ng/50,000 cells, using FuGeneHD (Promega) transfection reagent in Opti-MEM, as previously described (Rühl & Broz, 2015). In Fig 5B, LPS O111:B4 was transfected with Lipofectamine 2000. When indicated, BMDMs were treated with endocytosis inhibitors [80 μM dynasore (Sigma) or 3.0 mg ml^{-1} chlorpromazine (CPZ; Sigma)] for 30 min at 37°C before OMV stimulation. The farnesyl transferase inhibitor L-744,832 (Merck) was added at a concentration of 10 μM for 16 h (Modiano *et al*, 2005). The concentration of

all inhibitors was then maintained during the course of the experiment.

Generation of ΔCaaX GBPs and lentiviral transduction

Human GBP1, GBP2, and GBP5 lacking the C-terminal CaaX box were produced by mutagenesis. Briefly, ΔCaaX GBPs cDNAs were generated from wild-type cDNAs, by using the following primers: 5′-AGCACAGTGGCTCGAATGGCCTCCTACCCTTATG-3′ and 5′-GAGAGGGGCGGAATTTTATGCCTTTCGTCGTCTCATT-3′ (ΔCaaX-GBP1); 5′-AGCACAGTGGCTCGAATGGCCTCCTACCCTTATG-3′ and 5′-GAGAGGGGCGGAATTCTATATTGGCTCCAATGATTTGC-3′ (ΔCaaX-GBP2); 5′-AGCACAGTGGCTCGAATGGCCTCCTACCCTTATG-3′ and 5′-GAGAGGGGCGGAATTTTATGGATCATCGTTATTAACAGT-3′ (ΔCaaX-GBP5). Fragments were cloned into the lentiviral vector pAIP containing an HA-tag sequence at the N-terminal, after digestion with EcoRI and XhoI, using In-Fusion (Clontech) cloning technology. To produce lentiviral particles, 6×10^6 HEK293T cells were transfected with 17 μg lentiviral plasmid, 4.3 μg VSV-G, and 13 μg psPax2 for 4 h. Medium was exchanged, and lentiviral particles were collected 48 h later. U937 cells were spin-infected with these particles, and transduced cells were selected with puromycin (2 μg ml^{-1}, Invivogen) for 10 days. Selected cells were used for experiments.

siRNA-mediated knockdown

Genes were knocked down using GenMute (SignaGen Laboratories) and siRNA pools (siGenome; Dharmacon) as previously described (Meunier *et al*, 2015). After 72 h of gene knockdown, BMDMs were stimulated with purified OMVs and assessed for inflammasome activation.

Measurement of LDH and cytokine release and PI influx

Cell death was quantified by measuring LDH release, using the LDH Cytotoxicity Detection Kit (TaKaRa Clontech). To normalize for spontaneous cell lysis, the percentage of cell death was calculated as follows: [(LDH sample) − (LDH negative control)]/[(LDH positive control) − (LDH negative control)] × 100. The levels of IL-1β and IL-18 were measured by ELISA (eBiosciences), according to the manufacturer's instructions. PI influx measurement was performed as previously described (Rühl & Broz, 2015).

Western blotting analysis for inflammasome activation

For Western blotting of supernatant and lysate samples, BMDMs were seeded at 50,000 cells per well in 96-well plates. After stimulation, six wells were pooled and samples were processed as previously described (Dick *et al*, 2016). For combined supernatant and lysates, samples were prepared as above, but supernatant precipitates were resuspended in lysate samples. The following antibodies were used: rat anti-caspase-1 (Genentech, 1:1,000), rat anti-caspase-11 (clone 17D9, Sigma, 1:1,000), rabbit anti-IL-18 (5180R-100, Biovision, 1:1,000), goat anti-IL-1β (AF-401-NA, R&D, 1:1,000), rabbit anti-GBP2 (11854-1-AP; Proteintech, 1:1,000), rabbit anti-GBP5 (13220-1-AP; Proteintech, 1:1,000), mouse anti-GAPDH (AM4300; Life Technologies, 1:1,000) and mouse anti-β-actin (A1987, Sigma, 1:2,000). Secondary antibodies conjugated to horseradish peroxidase were used.

CCF4-AM assay

Bone marrow-derived macrophages were seeded into black 96-well glass bottom plates (Greiner), at a density of 40,000 cells per well, and then loaded with CCF4-AM substrate (LiveBLAzer FRET-B/G Loading Kit, Life Technologies) in FluoroBrite DMEM (Life Technologies) for 2 h at room temperature in the presence of 2.0 mM probenecid (Sigma), as previously described with modifications (Keller *et al*, 2013). Cells were washed, and $OMVs^{\beta\text{-lact}}$ were added in the presence of 2.0 mM probenecid. When necessary, 80 μM dynasore was added 30 min before $OMVs^{\beta\text{-lact}}$ stimulation, as described above. Fluorescence was measured using a plate reader, using the following filters (ex/em 405/550 and 405/420). FRET values were normalized to those when using OMVs not containing β-lactamase, to account for non-specific cleavage of the CCF4 probe.

Isolation of cytosolic fraction from BMDMs

Subcellular fractionation of OMV-treated BMDMs was performed using a differential digitonin-based fractionation method as previously described with modifications (Vanaja *et al*, 2016). Briefly, 2×10^6 cells (primed with LPS and IFN-γ) in a 6-well plate were washed four times and stimulated with 50 μg of OMVs for 2 h. Cells were washed four times with sterile cold PBS to remove extracellular OMVs, treated with 300 μl of 0.010% digitonin extraction buffer (0.010% digitonin, 10 mM HEPES pH 7.4, 300 mM sucrose, 100 mM NaCl, 3 mM $MgCl_2$, 5 mM EDTA, complete protease inhibitors) for 8 min, and the supernatant was collected (cytosolic fraction). The residual cellular fraction was then collected in 300 μl RIPA buffer. Cytosolic and residual fractions were subjected to BCA assay for protein quantification and LAL assay for LPS quantification (Thermo Scientific) according to the manufacturer's instructions. Fractionation was verified by Western blotting, using the following antibodies: rabbit anti-tubulin (Abcam, 1:1,000), mouse anti-GAPDH (AM4300; Life Technologies, 1:1,000), rat anti-Lamp-1 (homemade), rabbit anti-calnexin (Enzo Life Sciences, 1:1,000), rabbit anti-PDI (Enzo Life Sciences, 1:1,000), and rabbit anti-VDAC (CST, 1:1,000).

Quantitative PCR (qPCR)

mRNA was extracted from BMDMs and reversed transcribed into cDNA, and gene expression was quantified by qPCR using an iCylcer (Bio-Rad) and SYBER green (Applied Biosystems), according to standard protocols. The primers used are shown in Appendix Table S1.

Type I IFNs production measurement

Supernatants from OMV-treated BMDMs or the serum from OMV-injected mice were collected at the indicated time points. ISRE-L929 reporter cells were then used to measure type I IFNs levels as previously described (Peng *et al*, 2011). Briefly, ISRE-L929 cells were seeded at a density of 1×10^5 cells per well in black 96-well glass

bottom plates (Greiner) and allowed to adhere overnight at 37°C, 5% CO_2. Cells were then incubated with 60 µl of the collected supernatants or mice serum (diluted 10-fold). After 4 h, plates were equilibrated to room temperature, the supernatant was removed and the ISRE-L929 cells were lysed with 40 µl Glo lysis buffer (Promega) per well, for 5 min. 40 µl of Bright-Glo Luciferase Assay substrate (Promega) were then added, and after a 5-min incubation at room temperature, the luminescence levels were measured using a plate reader.

Immunofluorescence

Purified OMVs (at 1 mg ml^{-1}) were labeled by incubating them with 1% (v/v) Vybrant Dil (Life Technologies) for 20 min at 37°C. Unbound dye was then removed by doing three washes using a 100-kDa cutoff Vivaspin 500 ultrafiltration unit (GE Healthcare), and fluorescent OMVs were stored at 4°C for up to 6 weeks. As control, Vybrant Dil was added to PBS, and the procedure was repeated. BMDMs were seeded onto glass coverslips, primed with LPS and IFN-γ, and stimulated with fluorescently labeled OMVs. At the desired time points, cells were washed with PBS and fixed with 4% paraformaldehyde for 20 min at room temperature. Coverslips were then washed four times with PBS and incubated with 0.1 M glycine for 10 min at room temperature. Cells were permeabilized with 0.5% saponin for 10 min, blocked using 1% BSA and incubated with a rabbit anti-EEA-1 (CST, 1:100), rabbit anti-GBP5 (13220-1-AP; Proteintech, 1:100), or mouse anti-HA (Enzo Life Sciences, 1:500) antibodies. As secondary antibodies, Alexa Fluor 488-conjugated anti-rabbit or anti-mouse (Life Technologies, 1:500) was used. Coverslips were mounted on glass slides using ProLong Gold Antifade (Life Technologies) and imaged in a PerkinElmer UltraView spinning disk confocal microscope. *Z*-stacks of 200 nm step size were acquired using a 100×/1.45 NA oil objective. The following excitation lasers were used: 405, 488, and 561 nm. Fluorescence emission was detected with 445-nm (W60), 525-nm (W50), and 615-nm (W70) filters, respectively. Data were further analyzed and processed using Fiji software, and all derived images shown correspond to maximum 3D projections.

Streptavidin pulldown assays

Approximately 3×10^7 BMDMs were primed with LPS and IFN-γ. Cells were then collected and lysed in a buffer containing 50 mM Tris–HCl (pH 7.5), 150 mM NaCl, 5 mM EDTA, 1% NP-40, 0.05% Na-deoxycolate, and complete protease inhibitors. To determine LPS binding to endogenous caspase-11, 700 µg of protein from the total cell lysate was incubated overnight, at 4°C with constant rocking, with 2.0 µg biotinylated LPS or with 2.0 µg biotinylated LPS that has been pre-incubated with 1.0 µl FuGeneHD for 20 min at room temperature. 50 µl of streptavidin magnetic beads (Thermo Scientific) was washed in PBS with 0.05% Tween-20 and incubated with the resulting cell lysate for 2 h at room temperature with constant rocking. The beads were washed three times with PBS with 0.05% Tween-20 and once with PBS, and the precipitates were then eluted in 50 µl of SDS–PAGE reducing sample buffer followed by immunoblotting analysis. 20 µg of initial total cell lysate (input) and equal volumes of pulldown were analyzed.

Statistical analysis

Statistical analyses were performed in GraphPad Prism software v6, and significance was referred as *, **, ***, or **** for *P*-values < 0.05, < 0.01, < 0.001, or < 0.0001, respectively. For comparison of three or more groups, *P*-values were determined using the two-way analysis of variance test for multiple comparisons. For comparison of two groups, a two-tailed *t*-test was used. Animal experiments were evaluated using the Mann–Whitney or log-rank Cox–Mantel test (survival experiments).

Expanded View for this article is available online.

Acknowledgements
We would like to thank T. Roger, T. Calandra, M. Diamond, O. Neyrolles, and C. Kasper for reagents; all the members of the Broz group for fruitful discussions; Jaroslaw Sedzicki for technical assistance with electron microscopy; Mariana Martins for critical reading of the manuscript; and the Imaging Core Facility of the Biozentrum and the Center for Transgenic Models of the University of Basel, for technical assistance. This work was supported by the Swiss National Science Foundation (PP00P3_165893/1 to PB) and the Human Frontier Science Program (CDA00032/2015-C/2 to PB).

Author contributions
JCS, EM, and PB designed the study; BL, DD, KP, MY, PP, and TH provided essential mouse lines; JCS, MSD, EM, and PB performed experiments; JCS and PB wrote the manuscript.

Conflict of interest
The authors declare that they have no conflict of interest.

References

Aachoui Y, Leaf IA, Hagar JA, Fontana MF, Campos CG, Zak DE, Tan MH, Cotter PA, Vance RE, Aderem A, Miao EA (2013) Caspase-11 protects against bacteria that escape the vacuole. *Science* 339: 975 – 978

Acevedo R, Fernández S, Zayas C, Acosta A, Sarmiento ME, Ferro VA, Rosenqvist E, Campa C, Cardoso D, Garcia L, Perez JL (2014) Bacterial outer membrane vesicles and vaccine applications. *Front Immunol* 5: 121

Aglietti RA, Estevez A, Gupta A, Ramirez MG, Liu PS, Kayagaki N, Ciferri C, Dixit VM, Dueber EC (2016) GsdmD p30 elicited by caspase-11 during pyroptosis forms pores in membranes. *Proc Natl Acad Sci USA* 113: 7858 – 7863

Aurell CA, Wistrom AO (1998) Critical aggregation concentrations of gram-negative bacterial lipopolysaccharides (LPS). *Biochem Biophys Res Commun* 253: 119 – 123

Beutler B, Jiang Z, Georgel P, Crozat K, Croker B, Rutschmann S, Du X, Hoebe K (2006) Genetic analysis of host resistance: Toll-like receptor signaling and immunity at large. *Annu Rev Immunol* 24: 353 – 389

Bomberger JM, Maceachran DP, Coutermarsh BA, Ye S, O'Toole GA, Stanton BA (2009) Long-distance delivery of bacterial virulence factors by *Pseudomonas aeruginosa* outer membrane vesicles. *PLoS Pathog* 5: e1000382

Broz P, Newton K, Lamkanfi M, Mariathasan S, Dixit VM, Monack DM (2010) Redundant roles for inflammasome receptors NLRP3 and NLRC4 in host defense against *Salmonella*. *J Exp Med* 207: 1745 – 1755

Broz P, Ruby T, Belhocine K, Bouley DM, Kayagaki N, Dixit VM, Monack DM (2012) Caspase-11 increases susceptibility to *Salmonella* infection in the absence of caspase-1. *Nature* 490: 288 – 291

Chatterjee SN, Das J (1967) Electron microscopic observations on the excretion of cell-wall material by *Vibrio cholerae*. *J Gen Microbiol* 49: 1 – 11

Chen DJ, Osterrieder N, Metzger SM, Buckles E, Doody AM, DeLisa MP, Putnam D (2010) Delivery of foreign antigens by engineered outer membrane vesicle vaccines. *Proc Natl Acad Sci USA* 107: 3099 – 3104

Debierre-Grockiego F, Niehus S, Coddeville B, Elass E, Poirier F, Weingart R, Schmidt RR, Mazurier J, Guérardel Y, Schwarz RT (2010) Binding of *Toxoplasma gondii* glycosylphosphatidylinositols to galectin-3 is required for their recognition by macrophages. *J Biol Chem* 285: 32744 – 32750

Devoe IW, Gilchrist JE (1973) Release of endotoxin in the form of cell wall blebs during *in vitro* growth of *Neisseria meningitidis*. *J Exp Med* 138: 1156 – 1167

Dick MS, Sborgi L, Rühl S, Hiller S, Broz P (2016) ASC filament formation serves as a signal amplification mechanism for inflammasomes. *Nat Commun* 7: 11929

Ding J, Wang K, Liu W, She Y, Sun Q, Shi J, Sun H, Wang D-C, Shao F (2016) Pore-forming activity and structural autoinhibition of the gasdermin family. *Nature* 535: 111 – 116

Feeley EM, Pilla-Moffett DM, Zwack EE, Piro AS, Finethy R, Kolb JP, Martinez J, Brodsky IE, Coers J (2017) Galectin-3 directs antimicrobial guanylate binding proteins to vacuoles furnished with bacterial secretion systems. *Proc Natl Acad Sci USA* 114: E1698 – E1706

Fermino ML, Polli CD, Toledo KA, Liu F-T, Hsu DK, Roque-Barreira MC, Pereira-da-Silva G, Bernardes ES, Halbwachs-Mecarelli L (2011) LPS-induced galectin-3 oligomerization results in enhancement of neutrophil activation. *PLoS One* 6: e26004

Finethy R, Luoma S, Orench-Rivera N, Feeley EM, Haldar AK, Yamamoto M, Kanneganti T-D, Kuehn MJ, Coers J (2017) Inflammasome activation by bacterial outer membrane vesicles requires guanylate binding proteins. *MBio* 8: e01188–17

Guarda G, Braun M, Staehli F, Tardivel A, Mattmann C, Förster I, Farlik M, Decker T, Du Pasquier RA, Romero P, Tschopp J (2011) Type I interferon inhibits interleukin-1 production and inflammasome activation. *Immunity* 34: 213 – 223

Hagar JA, Powell DA, Aachoui Y, Ernst RK, Miao EA (2013) Cytoplasmic LPS activates caspase-11: implications in TLR4-independent endotoxic shock. *Science* 341: 1250 – 1253

Haldar AK, Piro AS, Pilla DM, Yamamoto M, Coers J (2014) The E2-like conjugation enzyme Atg3 promotes binding of IRG and Gbp proteins to Chlamydia- and Toxoplasma-containing vacuoles and host resistance. *PLoS One* 9: e86684

Haldar AK, Foltz C, Finethy R, Piro AS, Feeley EM, Pilla-Moffett DM, Komatsu M, Frickel E-M, Coers J (2015) Ubiquitin systems mark pathogen-containing vacuoles as targets for host defense by guanylate binding proteins. *Proc Natl Acad Sci USA* 112: E5628 – E5637

Hermann M, Cermak T, Voytas DF, Pelczar P (2014) Mouse genome engineering using designer nucleases. *J Vis Exp* 86: e50930

Irving AT, Mimuro H, Kufer TA, Lo C, Wheeler R, Turner LJ, Thomas BJ, Malosse C, Gantier MP, Casillas LN, Votta BJ, Bertin J, Boneca IG, Sasakawa C, Philpott DJ, Ferrero RL, Kaparakis-Liaskos M (2014) The immune receptor NOD1 and kinase RIP2 interact with bacterial peptidoglycan on early endosomes to promote autophagy and inflammatory signaling. *Cell Host Microbe* 15: 623 – 635

Jiang Z, Georgel P, Du X, Shamel L, Sovath S, Mudd S, Huber M, Kalis C, Keck S, Galanos C, Freudenberg M, Beutler B (2005) CD14 is required for MyD88-independent LPS signaling. *Nat Immunol* 6: 565 – 570

Kaparakis M, Turnbull L, Carneiro L, Firth S, Coleman HA, Parkington HC, Le Bourhis L, Karrar A, Viala J, Mak J, Hutton ML, Davies JK, Crack PJ, Hertzog PJ, Philpott DJ, Girardin SE, Whitchurch CB, Ferrero RL (2010) Bacterial membrane vesicles deliver peptidoglycan to NOD1 in epithelial cells. *Cell Microbiol* 12: 372 – 385

Kaparakis-Liaskos M, Ferrero RL (2015) Immune modulation by bacterial outer membrane vesicles. *Nat Rev Immunol* 15: 375 – 387

Kayagaki N, Warming S, Lamkanfi M, Vande Walle L, Louie S, Dong J, Newton K, Qu Y, Liu J, Heldens S, Zhang J, Lee WP, Roose-Girma M, Dixit VM (2011) Non-canonical inflammasome activation targets caspase-11. *Nature* 479: 117 – 121

Kayagaki N, Wong MT, Stowe IB, Ramani SR, Gonzalez LC, Akashi-Takamura S, Miyake K, Zhang J, Lee WP, Muszyński A, Forsberg LS, Carlson RW, Dixit VM (2013) Noncanonical inflammasome activation by intracellular LPS independent of TLR4. *Science* 341: 1246 – 1249

Kayagaki N, Stowe IB, Lee BL, O'Rourke K, Anderson K, Warming S, Cuellar T, Haley B, Roose-Girma M, Phung QT, Liu PS, Lill JR, Li H, Wu J, Kummerfeld S, Zhang J, Lee WP, Snipas SJ, Salvesen GS, Morris LX *et al* (2015) Caspase-11 cleaves gasdermin D for non-canonical inflammasome signalling. *Nature* 526: 666 – 671

Keller C, Mellouk N, Danckaert A, Simeone R, Brosch R, Enninga J, Bobard A (2013) Single cell measurements of vacuolar rupture caused by intracellular pathogens. *J Vis Exp* 76: e50116

Kesty NC, Mason KM, Reedy M, Miller SE, Kuehn MJ (2004) Enterotoxigenic *Escherichia coli* vesicles target toxin delivery into mammalian cells. *EMBO J* 23: 4538 – 4549

Kim B-H, Chee JD, Bradfield CJ, Park E-S, Kumar P, MacMicking JD (2016) Interferon-induced guanylate-binding proteins in inflammasome activation and host defense. *Nat Immunol* 17: 481 – 489

Kravets E, Degrandi D, Ma Q, Peulen T-O, Klümpers V, Felekyan S, Kühnemuth R, Weidtkamp-Peters S, Seidel CA, Pfeffer K (2016) Guanylate binding proteins directly attack *Toxoplasma gondii* via supramolecular complexes. *Elife* 5: e14246

Liu X, Zhang Z, Ruan J, Pan Y, Magupalli VG, Wu H, Lieberman J (2016) Inflammasome-activated gasdermin D causes pyroptosis by forming membrane pores. *Nature* 535: 153 – 158

Man SM, Karki R, Malireddi RKS, Neale G, Vogel P, Yamamoto M, Lamkanfi M, Kanneganti T-D (2015) The transcription factor IRF1 and guanylate-binding proteins target activation of the AIM2 inflammasome by *Francisella* infection. *Nat Immunol* 16: 467 – 475

Man SM, Karki R, Sasai M, Place DE, Kesavardhana S, Temirov J, Frase S, Zhu Q, Malireddi RKS, Kuriakose T, Peters JL, Neale G, Brown SA, Yamamoto M, Kanneganti T-D (2016a) IRGB10 liberates bacterial ligands for sensing by the AIM2 and caspase-11-NLRP3 inflammasomes. *Cell* 167: 382 – 396.e17

Man SM, Place DE, Kuriakose T, Kanneganti T-D (2016b) Interferon-inducible guanylate-binding proteins at the interface of cell-autonomous immunity and inflammasome activation. *J Leukoc Biol* 101: 143 – 150

Meunier E, Dick MS, Dreier RF, Schürmann N, Kenzelmann Broz D, Warming S, Roose-Girma M, Bumann D, Kayagaki N, Takeda K, Yamamoto M, Broz P (2014) Caspase-11 activation requires lysis of pathogen-containing vacuoles by IFN-induced GTPases. *Nature* 509: 366 – 370

Meunier E, Wallet P, Dreier RF, Costanzo S, Anton L, Rühl S, Dussurgey S, Dick MS, Kistner A, Rigard M, Degrandi D, Pfeffer K, Yamamoto M, Henry T, Broz P (2015) Guanylate-binding proteins promote activation of the AIM2

inflammasome during infection with *Francisella novicida*. *Nat Immunol* 16: 476 – 484

Meunier E, Broz P (2016) Interferon-inducible GTPases in cell autonomous and innate immunity. *Cell Microbiol* 18: 168 – 180

Mey A, Leffler H, Hmama Z, Normier G, Revillard JP (1996) The animal lectin galectin-3 interacts with bacterial lipopolysaccharides via two independent sites. *J Immunol* 156: 1572 – 1577

Modiano N, Lu YE, Cresswell P (2005) Golgi targeting of human guanylate-binding protein-1 requires nucleotide binding, isoprenylation, and an IFN-gamma-inducible cofactor. *Proc Natl Acad Sci USA* 102: 8680 – 8685

O'Donoghue EJ, Krachler AM (2016) Mechanisms of outer membrane vesicle entry into host cells. *Cell Microbiol* 18: 1508 – 1517

Pathirana RD, Kaparakis-Liaskos M (2016) Bacterial membrane vesicles: biogenesis, immune regulation and pathogenesis. *Cell Microbiol* 18: 1518 – 1524

Peng K, Broz P, Jones J, Joubert L-M, Monack D (2011) Elevated AIM2-mediated pyroptosis triggered by hypercytotoxic *Francisella* mutant strains is attributed to increased intracellular bacteriolysis. *Cell Microbiol* 13: 1586 – 1600

Pilla DM, Hagar JA, Haldar AK, Mason AK, Degrandi D, Pfeffer K, Ernst RK, Yamamoto M, Miao EA, Coers J (2014) Guanylate binding proteins promote caspase-11-dependent pyroptosis in response to cytoplasmic LPS. *Proc Natl Acad Sci USA* 111: 6046 – 6051

van der Pol L, Stork M, van der Ley P (2015) Outer membrane vesicles as platform vaccine technology. *Biotechnol J* 10: 1689 – 1706

Ramsby M, Makowski G (2011) Differential detergent fractionation of eukaryotic cells. *Cold Spring Harb Protoc* 2011: prot5592

Rathinam VAK, Vanaja SK, Waggoner L, Sokolovska A, Becker C, Stuart LM, Leong JM, Fitzgerald KA (2012) TRIF licenses caspase-11-dependent NLRP3 inflammasome activation by gram-negative bacteria. *Cell* 150: 606 – 619

Ray K, Bobard A, Danckaert A, Paz-Haftel I, Clair C, Ehsani S, Tang C, Sansonetti P, Tran GVN, Enninga J (2010) Tracking the dynamic interplay between bacterial and host factors during pathogen-induced vacuole rupture in real time. *Cell Microbiol* 12: 545 – 556

Rühl S, Broz P (2015) Caspase-11 activates a canonical NLRP3 inflammasome by promoting K(+) efflux. *Eur J Immunol* 45: 2927 – 2936

Sauer J-D, Sotelo-Troha K, von Moltke J, Monroe KM, Rae CS, Brubaker SW, Hyodo M, Hayakawa Y, Woodward JJ, Portnoy DA, Vance RE (2011) The N-ethyl-N-nitrosourea-induced Goldenticket mouse mutant reveals an essential function of Sting in the *in vivo* interferon response to *Listeria monocytogenes* and cyclic dinucleotides. *Infect Immun* 79: 688 – 694

Sborgi L, Rühl S, Mulvihill E, Pipercevic J, Heilig R, Stahlberg H, Farady CJ, Müller DJ, Broz P, Hiller S (2016) GSDMD membrane pore formation constitutes the mechanism of pyroptotic cell death. *EMBO J* 35: 1766 – 1778

Schwechheimer C, Kuehn MJ (2015) Outer-membrane vesicles from Gram-negative bacteria: biogenesis and functions. *Nat Rev Microbiol* 13: 605 – 619

Shenoy AR, Wellington DA, Kumar P, Kassa H, Booth CJ, Cresswell P, MacMicking JD (2012) GBP5 promotes NLRP3 inflammasome assembly and immunity in mammals. *Science* 336: 481 – 485

Shi J, Zhao Y, Wang Y, Gao W, Ding J, Li P, Hu L, Shao F (2014) Inflammatory caspases are innate immune receptors for intracellular LPS. *Nature* 514: 187 – 192

Shi J, Zhao Y, Wang K, Shi X, Wang Y, Huang H, Zhuang Y, Cai T, Wang F, Shao F (2015) Cleavage of GSDMD by inflammatory caspases determines pyroptotic cell death. *Nature* 526: 660 – 665

Takeuchi O, Akira S (2010) Pattern recognition receptors and inflammation. *Cell* 140: 805 – 820

Thurston TLM, Matthews SA, Jennings E, Alix E, Shao F, Shenoy AR, Birrell MA, Holden DW (2016) Growth inhibition of cytosolic *Salmonella* by caspase-1 and caspase-11 precedes host cell death. *Nat Commun* 7: 13292

Vanaja SK, Russo AJ, Behl B, Banerjee I, Yankova M, Deshmukh SD, Rathinam VAK (2016) Bacterial outer membrane vesicles mediate cytosolic localization of LPS and caspase-11 activation. *Cell* 165: 1106 – 1119

Wacker MA, Teghanemt A, Weiss JP, Barker JH (2017) High-affinity caspase-4 binding to LPS presented as high molecular mass aggregates or in outer membrane vesicles. *Innate Immun* 23: 336 – 344